



## **UTILIZATION OF COLD SEAWATER WITH HEAT PUMPS IN DISTRICT HEAT PRODUCTION**

Lappeenranta–Lahti University of Technology LUT

Master's Programme in Energy Technology Master's thesis

2022

Nita Huovilainen

Examiners: Professor, Esa Vakkilainen

Postdoctoral Researcher, Jussi Saari

Supervisor: M.Sc. (Tech), Laura Korhonen

## ABSTRACT

Lappeenranta–Lahti University of Technology LUT

LUT School of Energy Systems

Energy Technology

Nita Huovilainen

### **Utilization of cold seawater with heat pumps in district heat production**

Master's thesis

2022

83 pages, 57 figures, 1 table and 1 appendix

Examiners: Professor Vakkilainen Esa, Postdoctoral Researcher Jussi Saari

Supervisor: M.Sc. (Tech) Laura Korhonen

Keywords: Seawater heat pump, evaporator, heat exchanger, freezing fouling, biofouling

This master thesis discusses the effects of cold seawater on the seawater heat pump process in district heat production. This work is a literature study, so the results are based on literature or computational results. The work investigated the properties and effects of seawater in terms of freezing fouling, biological fouling and particle fouling. As the brackish water of the Baltic Sea is much less salty compared to the ocean, the freezing point is close to zero. However, the study deals with tenths of a degree, because they have a considerable effect on the usability of heat pumps and, through this, possibly on Helsinki's energy production. This study also dealt with various heat exchangers that are suitable as evaporators for heat pumps of industrial size. During the study, it was discovered that the shell-and-tube heat exchanger, could be suitable as an evaporator for a seawater heat pump. The shell-and-tube heat exchangers are a commonly used technology in industrial-sized heat pumps, and it is possible to manufacture the tube heat exchanger as a very pressure-resistant structure, even in a large size. The shell-and-tube heat exchanger enables reasonably easy cleaning. The most contaminated liquid should be placed on the side of the pipe so that it is easily accessible for mechanical cleaning. An automatic cleaning system, Taprogge, is available for the tube heat exchanger, so it is not necessarily open or clean chemically as often. There are also other heat exchanger options that can be considered for an industrial-sized seawater heat pump, for example falling film, diffusion bonded and plate-and-shell heat exchangers.

## TIIVISTELMÄ

Lappeenrannan–Lahden teknillinen yliopisto LUT

LUT Energiajärjestelmät

Energiatekniikka

Huovilainen Nita

### **Kylmän meriveden hyödyntäminen lämpöpumpuilla kaukolämmöntuotannossa**

Energiatekniikan diplomityö

2022

83 sivua, 57 kuvaa, 1 taulukko ja 1 liite

Tarkastajat: Professori Esa Vakkilainen, Tutkijatohtori Jussi Saari, Diplomi-insinööri Laura Korhonen

Avainsanat: Merivesilämpöpumppu, höyrystin, lämmönsiirrin, jäätyminen, likaantuminen

Tämä diplomityö käsittelee kylmän meriveden vaikutuksia merivesilämpöpumppuprosessiin kaukolämmön tuotannossa. Tämä työ on kirjallisuustutkimus, joten tulokset perustuvat kirjallisuuteen tai laskennallisiin tuloksiin. Työssä tutkittiin meriveden ominaisuuksia ja niiden vaikutuksia jäätyminen, biologisen likaantumisen ja partikkelilikaantumiseen. Itämeren ollessa murtoveittä ja vähemmän suolaista kuin valtameren vesi, jäätympiste on lähellä nollaa. Työssä kuitenkin käsitellään lämpötiloja asteen kymmenyksien tarkkuudella, koska niillä on huomattava vaikutus lämpöpumppujen käytettävyyteen ja sitä kautta Helsingin energiantuotantoon. Työssä käydään läpi erilaisia lämmönvaihtimia, jotka soveltuvat teollisuuden kokoluokan lämpöpumppujen höyrystimiksi. Putkilämmönvaihdin yleisesti käytetty tekniikka teollisuuden kokoluokan lämpöpumpuissa ja työssä huomattiin sen olevan sopiva myös merivesilämpöpumppukäyttöön. Putkilämmönvaihdin on mahdollista rakentaa erittäin paineenkestävistä rakenteista suuressa koossa ja putkirakenne mahdollistaa kohtuullisen helpon puhdistuksen. Putkilämmönvaihtimelle on saatavana automaattinen pallopuhdistusjärjestelmä, jota ei muille lämmönvaihdintyypeille vielä markkinoilta löydy. Putkilämmönvaihdin ei kuitenkaan kestä parhaiten jäätymistä, johon muut esitellyt lämmönvaihdintyypit sopivat paremmin.

## ACKNOWLEDGEMENTS

I have worked full time throughout my master's studies. Combining work, university and free-time has been challenging during my studies. I want to thank my whole family, especially my father, Tom, who made me excited about energy technology and has encouraged me during my studies. I also want to thank my boyfriend Ari-Markus, who has understood the challenges brought by my studies, even though sometimes I had lack of motivation and spent a lot of time with school assignments. Thanks also to my thesis supervisor and my co-worker Laura Korhonen. Laura spent many hours discussing with me about the master's thesis and I got a lot of good ideas from her. Now that I have finally finished my studies, I can take a breath and continue with new challenges.

## SYMBOLS AND ABBREVIATIONS

### Characters

$\Delta T_m$	average (mean) temperature difference	[°C, K]
$\mu$	dynamic viscosity	[Pa*s]
$A$	area	[m <sup>2</sup> ]
$c$	concentration	[mol/m <sup>3</sup> ]
$c_p$	specific heat	[J/kgK]
$d$	diameter	[m]
$D$	hydraulic diameter	[m]
$D_{AB}$	diffusion coefficient	[cm <sup>2</sup> s <sup>-1</sup> ]
$E_D$	eddy diffusion	[cm <sup>2</sup> s <sup>-1</sup> ]
$G$	Gibbs free energy	[J/mol]
$H$	enthalpy	[J/mol]
$h$	heat transfer coefficient	[W/m <sup>2</sup> K]
$i$	the van't Hoff factor	[-]
$k$	thermal conductivity	[W/mK]
$K_b$	ebullioscopic constant	[kg/mol]
$K_f$	cryoscopic constant	[kg/mol]
$L$	length	[m]
$\dot{m}$	mass flow	[kg/s]
$m$	molality	[mol/kg]
$N$	diffusion flux	[cm <sup>2</sup> s <sup>-1</sup> ]
$p$	pressure	[bar, Pa]

$q$	heat transfer rate	[W]
$Q_L$	thermal energy	[W]
$R$	resistance (convection or conduction)	[K/W]
$S$	entropy	[J/K]
$s$	salinity	[‰]
$T$	temperature	[°C, K]
$u$	mean velocity	[m/s]
$U$	overall heat transfer coefficient	[W/mK]
$U^*$	internal energy	[J]
$V$	volume	[m <sup>3</sup> ]
$W$	electrical work	[W]
$w$	wall thickness	[m]
$x$	molar fraction	[-]
$\gamma$	chemical potential	[J/kg]
$\Delta T_f$	freezing point depression	[°C, K]
$\rho$	density	[kg/m <sup>3</sup> ]
$\nu$	kinematic viscosity	[m <sup>2</sup> /s]

#### Dimensionless quantities

Re	Reynolds number
Pr	Prandtl number
Nu	Nusselt number

## Abbreviations

CFD      Computational Fluid Dynamics

COP      Coefficient of Performance

## Table of contents

Abstract

Acknowledgements

Symbols and abbreviations

1	Introduction .....	10
1.1	Background and purpose .....	10
2	Heat pumps and seawater process .....	11
2.1	Overview of the seawater process .....	11
2.2	Heat pump process in district heating production .....	12
2.2.1	Heat pump connection with intermediate circuit .....	14
2.2.2	Heat pump direct connection .....	15
3	Properties of seawater .....	17
3.1	Temperatures in the Baltic Sea .....	17
3.2	Oxygen content in the Baltic Sea .....	19
3.3	Salinity in the Baltic Sea .....	20
3.3.1	Freezing point depression .....	22
3.3.2	The effect of pressure on the freezing point .....	27
3.4	Seawater density .....	29
3.5	Thermocline and halocline .....	30
3.6	Characteristics of the seafloor .....	32
3.7	Characteristics of sea surface .....	35
4	Fouling of heat exchangers .....	37
4.1	Prevention of fouling .....	38
4.2	Heat transfer .....	39
4.3	Methods of fouling .....	46
4.3.1	Freezing .....	46
4.3.2	Particulate fouling .....	51
4.3.3	Biofouling .....	53
5	Case: Utilization of cold seawater in district heating production .....	57

5.1	Evaporator types.....	57
5.1.1	Shell and tube heat exchanger .....	58
5.1.2	Falling film heat exchanger .....	60
5.1.3	Diffusion bonded heat exchangers.....	61
5.1.4	Plate and shell heat exchanger .....	63
5.2	Evaporator the Degree of approach.....	64
5.2.1	Tube wall temperature and ice layer .....	67
5.2.2	Effect of seawater temperature on power .....	70
5.3	Filters.....	72
5.3.1	Seawater filtration methods .....	72
5.3.1.1	Seawater intake without subsea filtration .....	73
5.3.1.2	Subsea filtration .....	75
5.3.1.3	Seawater filters at the facility.....	78
6	Conclusions .....	80
	References.....	83

# 1 Introduction

Helsinki's goal is to be carbon neutral by 2030. The burning of coal in Helsinki will end in 2029, and as a result, the Salmisaari coal power must be replaced alternative energy sources. Electricity production does not have to be done in Salmisaari, even part of the production will stay in Salmisaari after coal is removed, for example a pellet boiler. The urban area has a district heating network and producing district heat in another location would cause losses, therefore local heat production must be secured in the future. One of the options under consideration is the seawater heat pumps to which this study relates.

## 1.1 Background and purpose

The purpose of the study is to investigate the challenges of cold seawater ( $\sim 2\text{--}0\text{ }^{\circ}\text{C}$ ) in the seawater heat utilization process. The seawater process is related to a seawater project that aim is to produce 475 MW thermal energy in the form of district heat utilizing seawater heat pumps using seawater heat. The aim of the study is to find out the challenges of the seawater process so that the operational reliability and availability of the seawater process and the heat pump can be maintained at a good level throughout the life cycle of the plant.

The study is looking for solution to the challenges of the seawater process, such as how freezing and fouling occur with cold seawater and how these can be prevented. The research also gathers information about the properties of the Baltic Sea and the challenges posed by cold seawater in the heat pump process. The study compares different evaporators because they have a large effect on the size, power, fouling, and freezing of the heat pump.

The research questions are,

- Challenges posed by fouling in the seawater process
- Challenges posed by cold seawater and freezing in the heat pump process

## 2 Heat pumps and seawater process

Normally we are used to the heat transfer from warm to cold and this happens in nature without any auxiliaries. The reverse process, in which heat energy is transferred from a colder state to a warmer state, cannot happen by itself, but requires a device called a heat pump.

### 2.1 Overview of the seawater process

The study examines the most difficult time for seawater heat recovery, when the seawater temperatures are at their coldest, around 0-2 °C. In winter the seawater would be taken along a 17-27 km tunnel from a depth of 50-70 meters and in summer the seawater would be taken from a surface. This study examines the seawater qualities at the both depths and investigate the cold seawater challenges. The study does not consider costs or profitability calculation. The place of seawater intake affects the seawater properties such as nutrients, salinity, temperature and oxygen content. (Helen, 2022) Several alternative implementations have been made for seawater tunnels and Figure 1 shows a couple of them. The water intake tunnel leaves from the Salmisaari power plant area, where the heat pump plant is planned to be built and ends at a depth of 50-70 meters in the Baltic Sea at 17-27 km. In the figure 1 is the vedenottotunneli 1 which is a 17 km tunnel and a water intake point at a depth of 50 meters. The second option, vedenottotunneli 2 is a 27 km tunnel and a water intake point at a depth of 70 meters. The third option is to use coast shore only without tunnel. The seawater tunnel has not yet been implemented but will have to be drilled if a 475 MW heat pump plant is to be built.

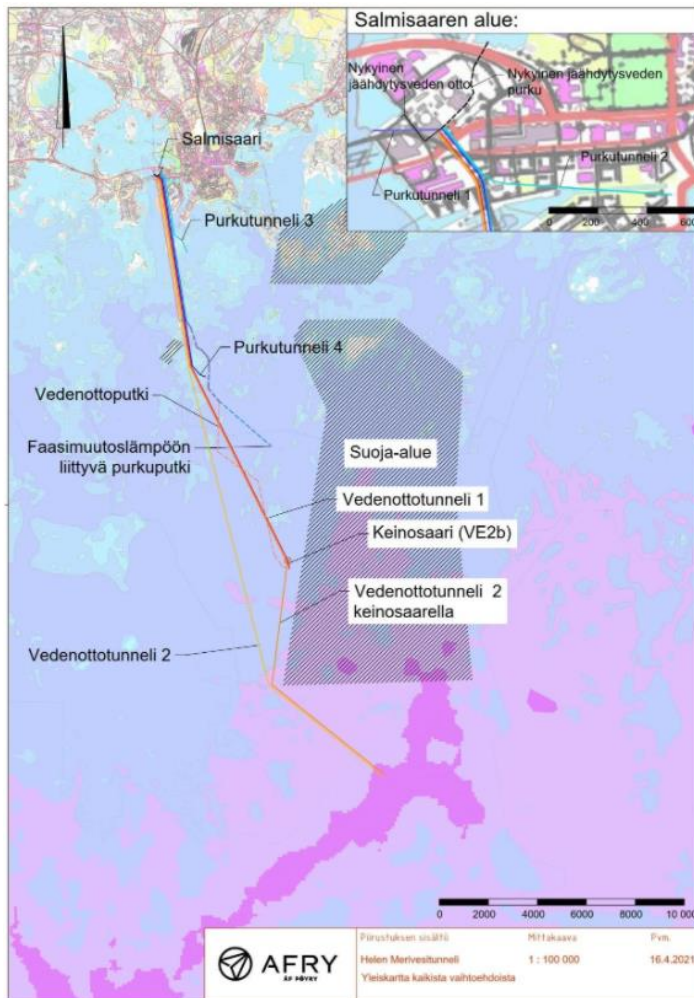


Figure 1 Afry's report on the seawater tunnel (Helen Oy, 2022)

## 2.2 Heat pump process in district heating production

In the heat pump solution under consideration, a refrigerant is used as the medium and the heat energy contained in the seawater is used as the heat source, which is fed into the district heating network. The temperature of the return district heating water is approx. 40 °C, which is raised to approx. 95 °C in the winter time, where the temperature difference is 55 °C. The study assumes that the heat taken from the sea is as low as possible and the study uses seawater between approx. 0-2°C. The temperature of the seawater returned to the sea will be determined in this study, as cold as possible. The seawater flow is a compromise between the investment cost and the heat pump plant usability. The maximum seawater flow together with the available temperature difference determines the instantaneous power available from

the plant. Decreasing the temperature difference increases the required heat transfer area and water mass flow. The intended district heating power is approx. 475 MW, and the efficiency of the heat pump plant determines the power required from seawater.

In the heat pump process under the critical point, the refrigerant vapor is pressurized to a higher pressure in the compressor and the refrigerant heats up. The refrigerant vapor is transferred to a condenser, where the refrigerant condenses into a liquid, releasing thermal energy to the district heating water. The high-pressured refrigerant goes to the expansion valve, where temperature and pressure drop. The refrigerant enters the evaporator as a liquid / gas mixture and absorbs the thermal energy from the sea (or district cooling network). The seawater cools and the refrigerant continues to the compressor starting from the beginning of the cycle.

The efficiency of the heat pump is determined by the COP-value (Coefficient of Performance).  $COP_R$  determines the ratio of the amount of cooling and  $COP_{HP}$  determines the ratio of the amount of heating to the work used (equation 1). The aim of the case is to maximize heat production, which means that higher  $COP_{HP}$  lead to higher efficiencies. When district heating water is 95 °C and seawater is 1 °C, the COP is approx. 2,6-2,7. The COP value varies according to the type of heat pump and the refrigerant used, but this COP value was estimated by one heat pump supplier. (Helen Oy, 2022) The COP increases as the temperature difference between the evaporator and the condenser decreases and the COP decreases as the temperature difference increases. As a rule of thumb, the COP rises from two to four percent of each degree as the temperature in the evaporator rises or the temperature in the condenser lowers. (Cengel, 2020)

$$COP_{HP} = \frac{Q_L}{W} \quad (1)$$

where  $COP_{HP}$  is Coefficient of Performance [-],  $Q_L$  is thermal energy [W] and  $W$  is electrical work [W]

Heat pumps must be suitable for the conditions of the heat source and the area to be heated or cooled, taking into account the temperature ranges and the dynamics of the process. The

temperature of the condenser can change due to the load on the district heating system and rapid fluctuations in the district heating or cooling network. Those fluctuations can also cause heat pump shutdowns. During power plant start-ups and rundowns, the flows in the district heating network can change drastically. In particular, the rapid decrease in flow means that the heat pump is not kept up. Industrial-grade heat pumps are often designed for smooth operation, with continuous starts and stops straining equipment, which can lead to shorter component life and increased failure. (Komulainen, 2022)

### 2.2.1 Heat pump connection with intermediate circuit

The heat pump can be connected to the seawater system directly or with an intermediate circuit. Figure 2 shows the principle of connecting a heat pump to a seawater system using an intermediate circuit. When the district heating capacity of a heat pump plant is 475 MW and the COP of the heat pump is assumed to be 2,6, the required glycol flow can be calculated to be about 50,000 m<sup>3</sup>/h. Glycol would be needed quite a bit in the intermediate circuit. Because the pipeline would be hundreds of meters long, for example, 300 meters of this line would require approx. 1000 m<sup>3</sup> of glycol. The amount of pumping would also increase, as the glycol side would need its own pumps and the overall COP of the heat pump would deteriorate due to increasing electricity need.

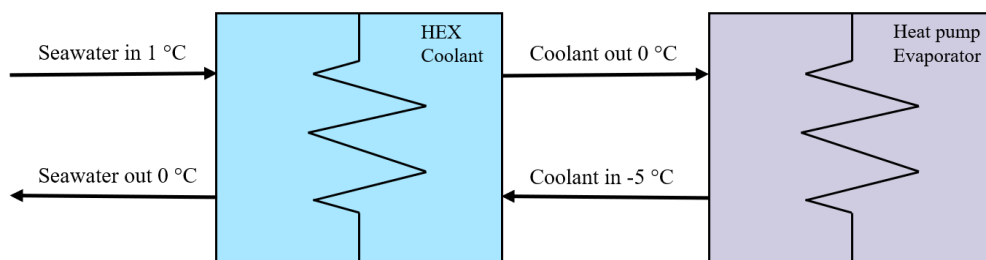


Figure 2 Heat pump connection with intermediate circuit

The intermediate circuit also brings benefits to the process. It would be possible to run heat pumps with very cold seawater, as the  $dT$  of the heat pump evaporator could be kept higher

( $dT$  5 Kelvin drawn in the figure) because the glycol does not present a risk of freezing to the evaporator. In this way the operating season will certainly last longer, even if the seawater temperature drops close to zero. In this case, minus degree glycol would go to the seawater heat exchanger and the risk of freezing would be existing in there. However, the evaporator of an industrial-sized heat pump has thousands of kilograms of refrigerant and the evaporator is a more valuable component than a seawater exchanger, so there the risk of freezing is better to have in the seawater exchanger than evaporator. When the  $dT$  of the evaporator is higher, a smaller heat transfer area is required, resulting in a smaller evaporator.

The biggest benefit of this system is at low seawater temperatures. The main benefits of an intermediate circuit system are the cleaning of the evaporators, the reduction of the corrosive and the cheaper choice of materials. In this case, the fouling heat exchanger can be chosen more from the point of view of fouling prevention (suitable type and flow technical properties) and there is no need to consider its suitability as an evaporator. But pumping costs increase, technology and the associated costs, the investment cost is estimated to be higher with the glycol system and maintenance costs increase.

### 2.2.2 Heat pump direct connection

The evaporator of the heat pump can also be connected to the sea by direct connection (figure 3). In direct connection, seawater is taken directly to the evaporator without a separate intermediate circuit. There is a risk of freezing and fouling in the evaporator in a direct seawater connection. When the temperature of the incoming seawater is 1-2 °C, it should be cooled in the evaporator close to the freezing point. The material costs of the evaporator also increase, the evaporator must be made of a material that can certainly withstand the corrosive properties of seawater, for example titanium. If the evaporator breaks down due to freezing or corrosion and the refrigerants escape, this means refrigerant loss of up to hundreds of thousands of euros, environmental harm and very high repair costs for the evaporator.

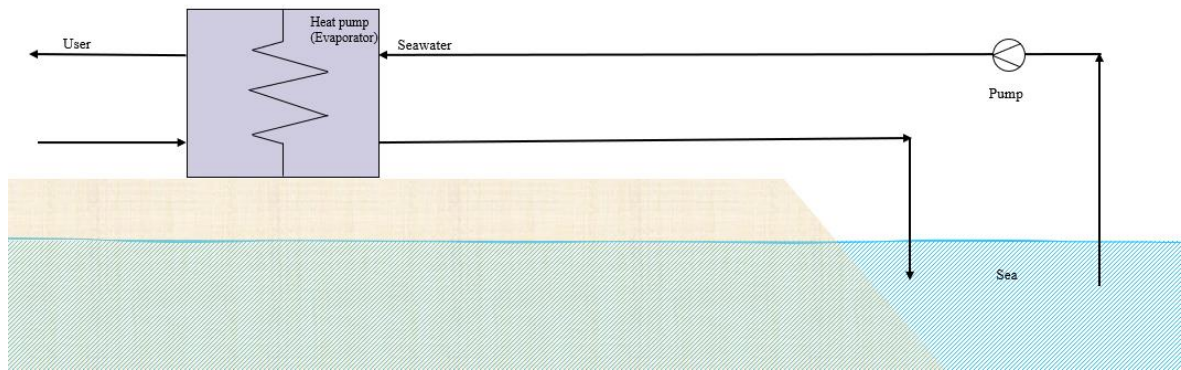


*Figure 3 Heat pump direct connection to the sea*

The biggest benefit of direct connection is lower pumping costs and the energy contained in seawater can be more efficiently transferred to the heat pump (there are no extra heat exchangers wasting energy). There is also no need to invest in the intermediate circuit and the intermediate circuit does not take up space.

### 3 Properties of seawater

The following section shows the properties of seawater in surface water and groundwater. The Baltic Sea is described in this work in order to understand the risk factors related to seawater heat recovery and the resulting technical challenges at a sufficient level. The properties of surface water are taken from the report of the Environmental Monitoring and Control Unit of the Helsinki Urban Environment 2018-2019. Groundwater data has been retrieved through the itämeri.fi website, which has been implemented in cooperation with several environmental operators. The data is read from a depth of 53 m from the Länsi-Tonttu measuring point, which is located in the Gulf of Finland near Helsinki. The study shows the temperature and salinity distributions for February and August (data retrieved from the reference Myrberg et al., 2006).

#### 3.1 Temperatures in the Baltic Sea

In summer, the surface water in the high seas is usually 15 to 20 °C in the Gulf of Finland. During long warm periods, the coastal waters can warm well over 20 °C. Surface water temperature varies greatly depending on the season and weather conditions. Surface water temperature ranges from 0,5 °C to 17 °C during the years 2003-2018. The measurements are shown in the figure 4 and have been taken on the Länsi-Tonttu in Helsinki. The coldest surface water is in February-March and warmest between July-August. The warmest surface water is in late summer/early autumn. The measurement site is a few kilometres from Salmisaari. However, these measurements provide direction only for temperature variations. (Itämeri.fi, 2022)

## Helsinki, Länsi-Tonttu

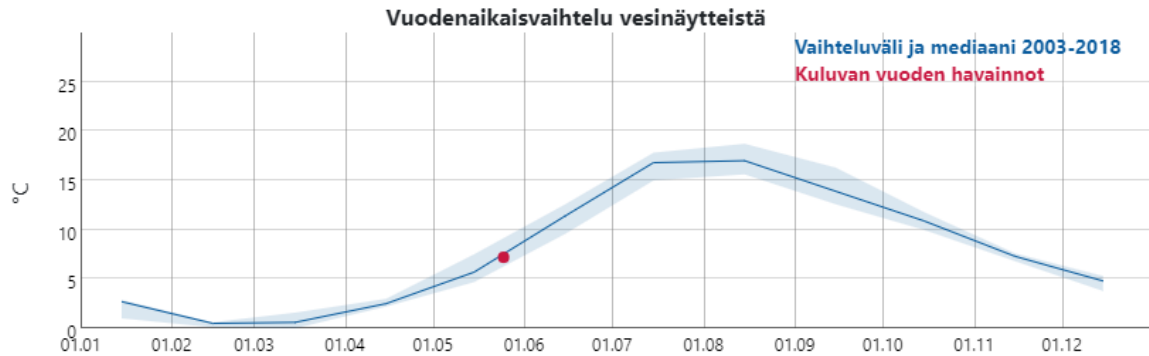


Figure 4 Helsinki, Länsi-Tonttu surface temperatures (Itämeri.fi, 2022)

Figures 5 and 6 shows the stratification of temperatures in the Baltic Sea in February and August. As can be seen from the figure 5, the seawater in the Gulf of Finland at a depth of 50 meters is approx. 1 °C in February. Going deeper into the Gulf of Finland, at a depth of 70 meters the temperature is approx. 3 °C. Winter data must be examined separately for each water intake site, because seawater temperature lowers close to freezing point. In August, the seawater temperature in 50 meters is approx. 3 °C, but then the surface temperature of the water is approx. 17 °C, as mentioned earlier, so it is more sensible to take water from the surface. In this case, the pumping cost is lowered when the  $dT$  of the water is higher. (Myrberg et al., 2006)

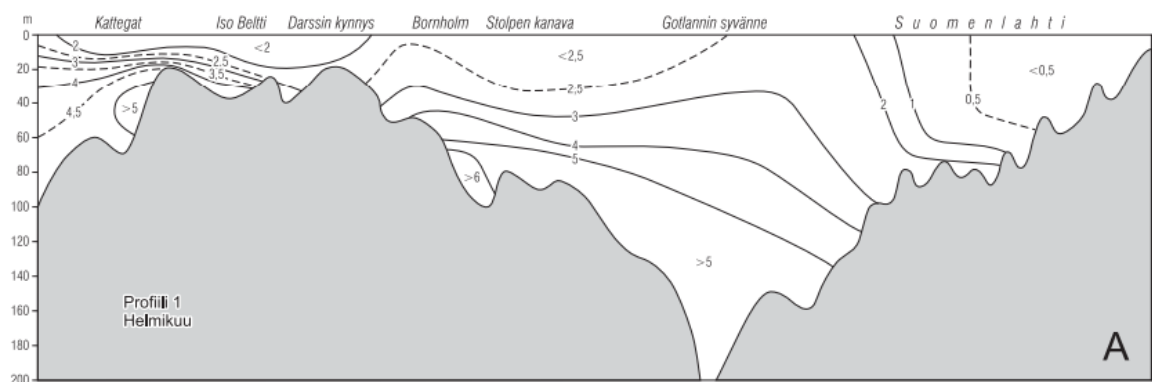


Figure 5 Temperature stratification of the Baltic Sea in February (Myrberg et al., 2006)

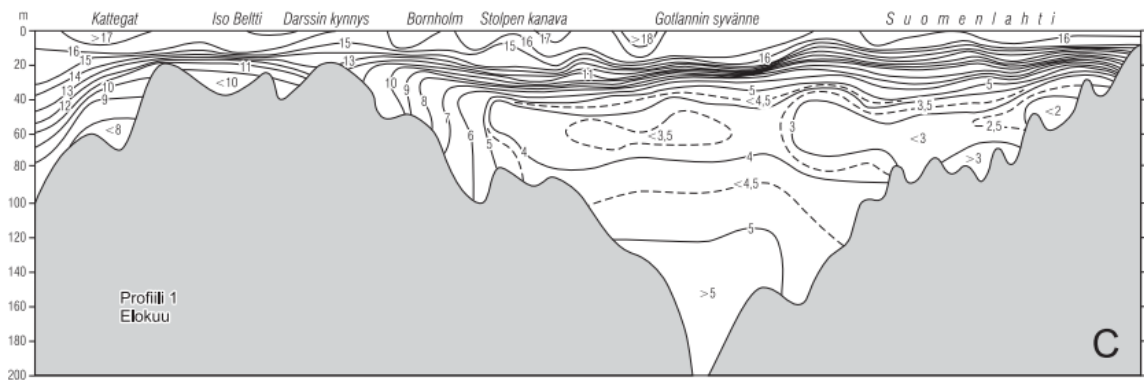


Figure 6 Temperature stratification of the Baltic Sea in August (Myrberg et al., 2006)

### 3.2 Oxygen content in the Baltic Sea

Oxygen is dissolved in water. In the deepest parts of the Gulf of Finland, the oxygen concentration is often below 2 ml/l, and this is too little for many organisms. Figure 7 shows that at a depth of 53 meters at the Länsi-Tonttu measuring point, the oxygen concentration is at its lowest at approx. 7 mg/l. This gives some indication that there is probably oxygen at a depth of 50 meters although not as much as at sea level. Loss of oxygen often occurs in winter, when ice prevents oxygen from dissolving in the water. There can also be problems in the summer, when the temperature difference between the surface and the bottom is so large that the water layers do not mix, and oxygen cannot reach the deepest layers. Especially at the end of summer, oxygen can completely run out of water. The main basins of the Baltic Sea are almost permanently oxygen-free, as shown in figure 8 and at a depth of 70 meters, lack of oxygen is likely. (Itämeri.fi, 2018) Oxygen is a prerequisite for life even in water. If the bottom runs out of oxygen, benthic animals will disappear, and the bottom will become desolate. As the situation continues, the lack of oxygen spreads to even higher water layers.

Spring and autumn will solve the problem, then the so-called full cycle mixes the water layers of the sea and brings new oxygenated water near the bottom. (vesi.fi, 2019)

### Helsinki, Länsi-Tonttu

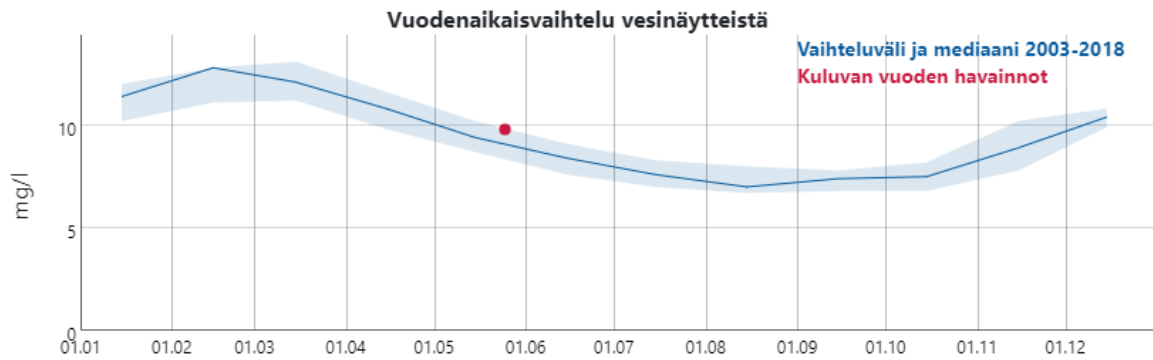


Figure 7 Länsi-Tonttu oxygen content, depth 53 m (Itämeri.fi, 2018)

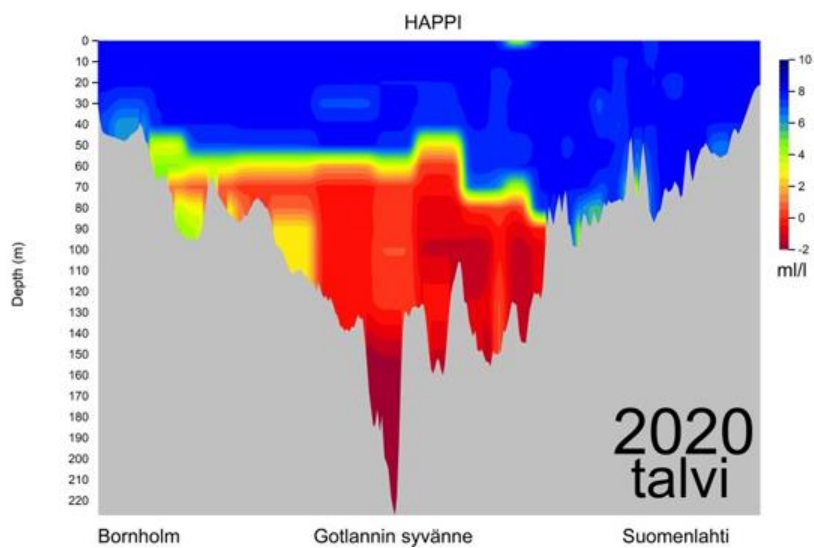


Figure 8 Cross-sectional view of the oxygen content of the Baltic Sea (Suomen ympäristökeskus, 2020)

### 3.3 Salinity in the Baltic Sea

The surface water salinity is the highest in the outer archipelago. During the winter months it is about 5,7 ‰ and decreases towards summer to 5,2 ‰ (figure 9). Closer to the coast salinity is the opposite. The drain from land lowers the salinity of surface water near the coast early in the year and the impact recently extends into the outer archipelago during summer. After the autumn, the salinity of the surface water of the outer archipelago returns

higher. In the outer archipelago of the Gulf of Finland, the salinity of water is affected by wind conditions and their variations. The wind moves the surface of the sea, as the wind blows from the east. Water flows from the Gulf of Finland to the middle of the Baltic Sea which brings water from the deepest layers of water in the middle of the Baltic Sea. When the winds blow from the west, the vertical stratification of the water decreases, the flow from deep water decreases. When the vertical stratification is weaker, the salinity of the water on the coasts is usually higher. (Helsingin kaupunki, 2020)

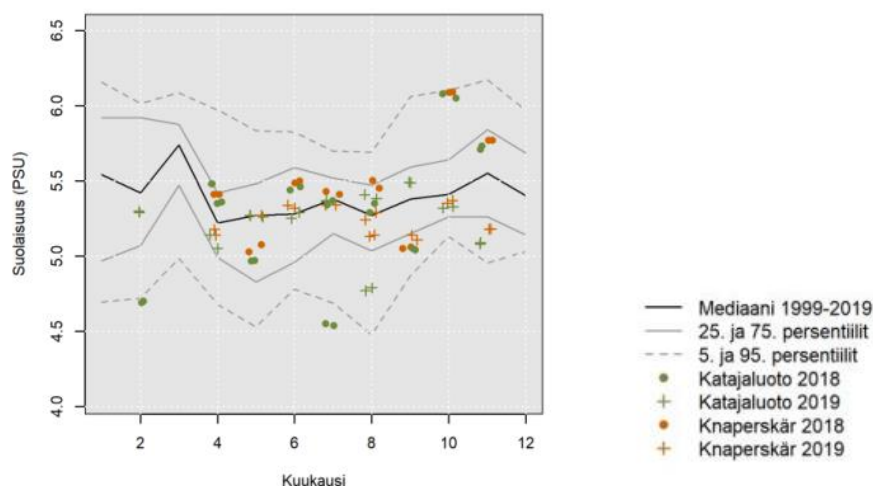


Figure 9 The surface water salinity (Helsingin kaupunki, 2020)

The average salinity of seawater is 3,5 %. The low-salinity water of the Baltic Sea is called brackish water because it has different properties from the ocean. Fresh water flows from the rivers into the Baltic Sea, but the salty ocean water can only enter the Baltic Sea through the shallow straits of Denmark. The inflowing water is saltier and heavier than the water of the Baltic Sea and therefore sinks into deep layers. (Suomen ympäristökeskus, 2022). In the deepest aquifers, relatively strong salinity stratification may occasionally occur, leading to relatively high-density differences between surface and bottom waters (>3 kg/m<sup>3</sup>). During the summer, the water is also heavily stratified because of temperature. During the strongest stratification, the water does not mix to the bottom, so that the nutrient reserves of the deepest water layers do not end up in the surface aquifer and the oxygenated surface water does not mix deeper. (Helsingin kaupunki, 2020) The saltiest area of the Baltic Sea is found in the

depths of Gotland. The seawater in the Baltic Sea in the Danish Straits is about 20 ‰ and will decrease further Baltic Sea. In the figures 10 and 11 is seen salt stratifications. The figure shows the salinity stratification in the Baltic Sea. In the figure, the salinity in the Gulf of Finland at a depth of 50 meters is about 6-7 ‰, depending of the of the season. The study uses 0-10 ‰ salt concentrations in the calculation and 5-8 ‰ salt concentrations are studied in more detail.

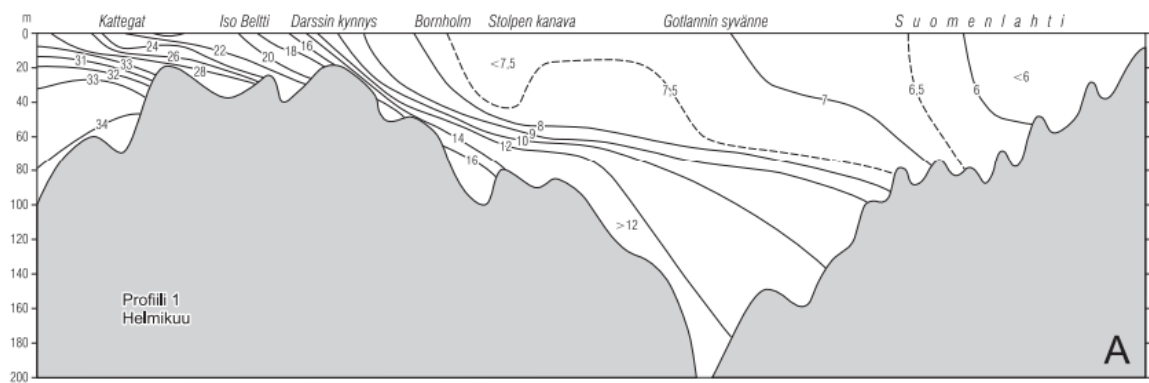


Figure 10 Salinity content of the Baltic Sea in February (Myrberg et al., 2006)

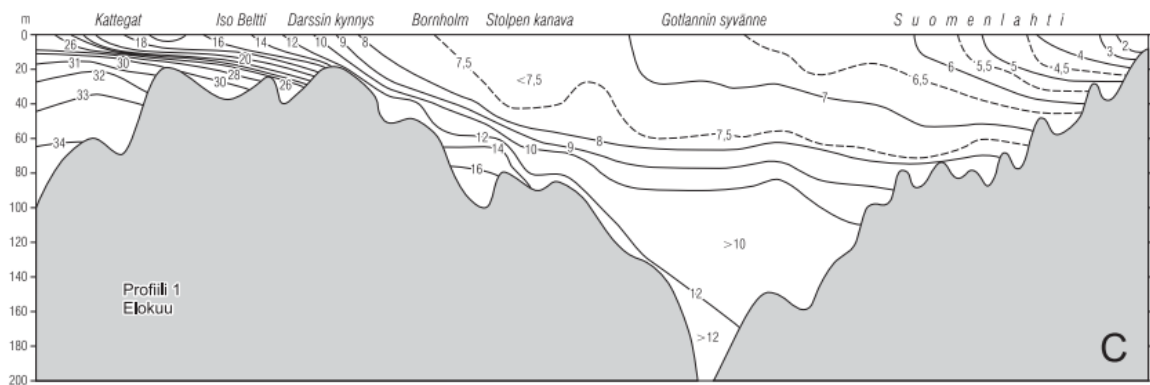


Figure 11 Salinity content of the Baltic Sea in August (Myrberg et al., 2006)

### 3.3.1 Freezing point depression

The temperature when a pure liquid freezes or changes to a crystalline solid is called freezing point. When the same happens the opposite, is called the melting point. The phase transition, in this case freezing or melting happens in steady temperature, with pure water at 0 °C. When

salt is added to water, freezing point decreases and this is called freezing point depression. Freezing point depression describes why the solute adding to solvent lowers the freezing point. When freezing starts, the molecules slows due the decrease in temperature and the liquid turns solid.

Seawater salt is mainly sodium chloride dissolved from rock and soil. By default, the calculations assume that the solution contains only sodium chloride and water. The amount of sodium chloride is 5 to 8 ‰. The freezing point depression can be calculated with equations 3a and 3b.

$$\Delta T_f = i K_f m \quad (3a)$$

$$m = \frac{\text{moles of NaCl}}{\text{kilograms of water}} \quad (3b)$$

where  $\Delta T_f$  is the freezing point depression [ $^{\circ}\text{C}$ , K],  $i$  is the van't Hoff factor,  $K_f$  is the cryoscopic constant for the solvent (for water is  $1,86 \text{ }^{\circ}\text{C kg mol}^{-1}$ ) and  $m$  is the molality of the solution [mol/kg]. Using the same equation, it is possible to determine the boiling point elevation if the constant  $K_f$  is replaced by a constant  $K_b$  which is the ebullioscopic constant (for water is  $0,52 \text{ }^{\circ}\text{C kg mol}^{-1}$ ). (Mullin, 2001)

The van't Hoff factor is the number of moles of particles when 1 mole of a solute dissolves and it is determined according to whether the mixture contains electrolytes. For example, sugar is not an electrolyte and does not decompose in water. Adding a mole of solid sugar gives a mole of dissolved sugar molecules. Electrolytes such as NaCl dissociate to ions ( $\text{NaCl} \rightarrow \text{Na}^+ + \text{Cl}^-$ ). Decompose one mole of NaCl gives two moles of dissolved particles, 1 mol of  $\text{Cl}^-$  and 1 mol of  $\text{Na}^+$ . So van't Hoff factor is 2. (Jyväskylän yliopisto, 2010)

With equations 3a and 3b the freezing point depression is for the water which has 5 to 8 ‰ salinity content is between  $0,32 \text{ }^{\circ}\text{C}$  and  $0,51 \text{ }^{\circ}\text{C}$ . At normal atmospheric pressure, water freezes at  $0 \text{ }^{\circ}\text{C}$ , with previously mentioned salt content to  $-0,3$  to  $-0,5 \text{ }^{\circ}\text{C}$ . The freezing point as a function of salinity is shown in the figure 12.

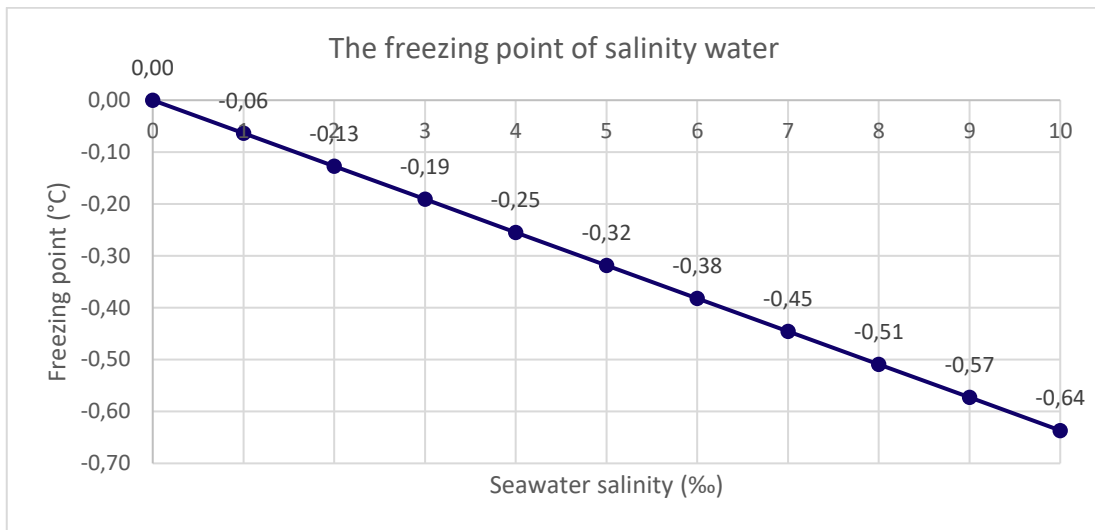


Figure 12 The freezing point as a function of salinity

A figure 13 phase diagram is for pure solvent and solution. Impurity addition to the solvent lowers the vapor pressure of the liquid, which lowers the freezing point  $T_f$  of the solution and raises the boiling point  $T_b$ .

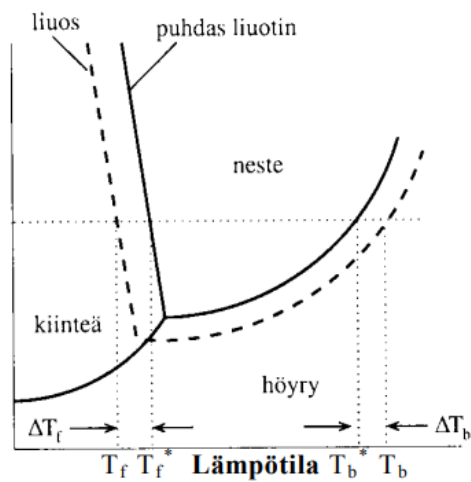


Figure 13 Phase diagram (Jyväskylän yliopisto, 2010)

In a figure 14 is a chemical potential as a function of temperature. When an impurity is added to a pure solvent, the chemical potential of the liquid phase decreases, resulting in a decrease in the freezing point and an increase in the boiling point. The slope of the graph describes the molar Gibbs energy of the system, which is always greater for gas than for liquid. At a given temperature, the most stable phase is always the one with the lowest chemical

potential. The chemical potential of the solution can be calculated by the equation 4. Since  $x_{\text{solvent}} < 1$ , the chemical potential of the solution is lower than the pure solvent. It is assumed that only the chemical potential of the liquid phase decreases, as it is only affected by the dissolved substance. In other words, the dissolved substance does not evaporate when the liquid boils and does not crystallize when the liquid freezes. (Jyväskylän yliopisto, 2010)

$$\gamma = \gamma^* + RT \ln(x_{\text{solvent}}) \quad (4)$$

where  $\gamma$  is the chemical potential of the solution [J/mol],  $\gamma^*$  is the chemical potential of the pure substance [J/mol],  $x$  is the molar fraction of solvent [-],  $R$  is the universal gas constant 8,314 [J/K mol] and  $T$  is the temperature of solution [K].

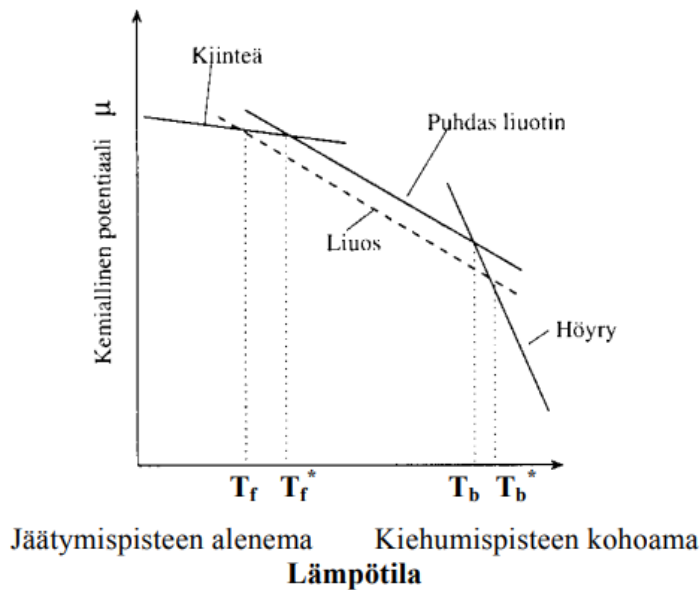


Figure 14 Chemical potential as a function of temperature (Jyväskylän yliopisto, 2010)

Figure 15 shows the phase diagram for salt water with dissolved salt (NaCl). The eutectic composition of water and salt is about 27 wt % salt dissolved in water. The eutectic point means the melting or freezing temperature is as low as possible and with saltwater it is - 21,1 °C. A maximum of about 30% of salt can be dissolved in water, and the temperature slightly

increases the salt's solubility. If the salt concentration is lower than the eutectic concentration, the water freezes into salt-free ice and the salt concentration of liquid water increases. As you can see, the red point in the figure has about 18% salt, so the liquid has about 24% salt and the ice is salt-free. (Institutes of the Faculty of Engineering, 2022) There is about 5-8 % salt in the Baltic Sea, but the same thing happens here. When salt water begins to freeze, pure ice and water with a higher salt content than before partial freezing are formed. The saltwater ice does not exist at these concentrations, so the density of the resulting ice is the same as the density of ice formed from pure water. For the same reason, the same amount of energy is released as when pure water freezes. (Laitinen, 2022)

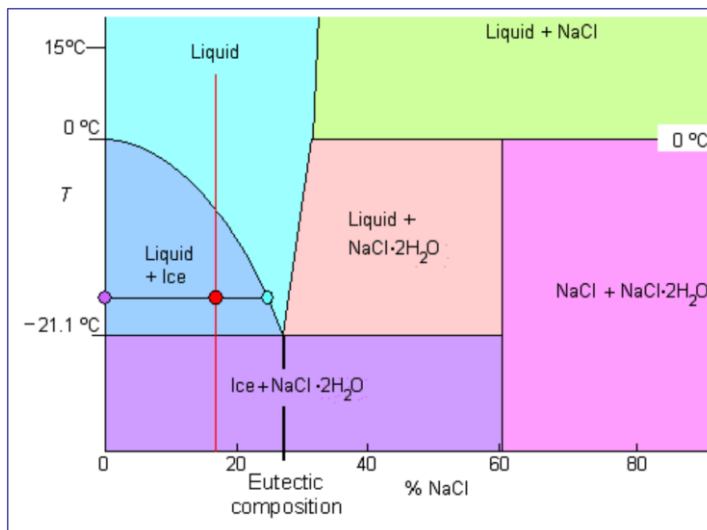


Figure 15 Phase diagram of salt water (Institutes of the Faculty of Engineering, 2022)

The vapor pressure of a liquid describes the tendency of liquid molecules to move from liquid to gas. In the case of a solution with water and salt, fewer solvent molecules can be transferred from the liquid to the gas. This is illustrated in Figure 16. In this case, the vapor pressure of the solution is lower than that of the pure solvent. The dissolved substance also increases the entropy of the solution, whereby the tendency of the liquid to form a gas decreases, then the boiling point increases. Increased disorder in the solution also reduces freezing and it causes the freezing point depression.

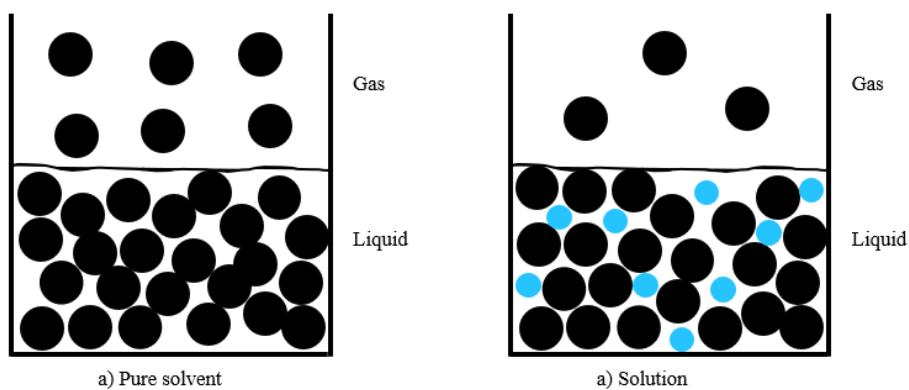


Figure 16 Effect of the impurity on the vapor pressure

### 3.3.2 The effect of pressure on the freezing point

Boiling point does change due the pressure changes, but the melting point are affected only by large pressure changes. Figure 17 shows a phase diagram of water, and the effect of pressure on the boiling point or freezing point can be seen from the graph. There is a connection between temperature and pressure, when the pressure drops, the boiling point of the water decreases rapidly, and the freezing point decreases slightly. A yellow arrow is drawn on the graph to show the change in boiling point and a blue arrow is drawn to show the change in freezing point as the pressure decreases. As can be seen from this figure 17, the pressure does not affect the freezing point dramatically and in many cases, it can be ignored.

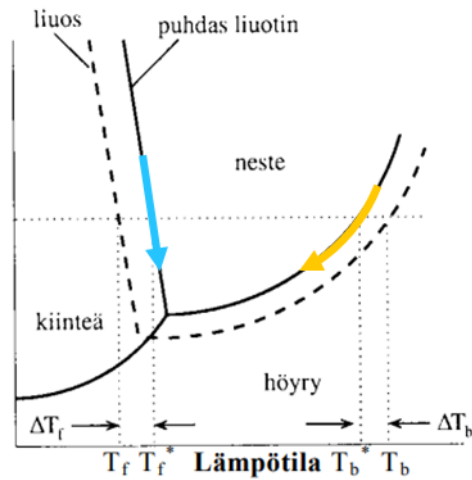


Figure 17 Phase diagram of water (Jyväskylän yliopisto, 2010)

At the liquid-gas and liquid-solid coexistence curves Gibbs free energy of one phase is equal to the free energy of another phase. Since the Gibbs free energies are equal on the coexistence curves, it is possible to use the change of Gibbs free energies to define pressure or temperature changes. The Gibbs free energy is defined by internal energy and entropy in an equation 5. (Ebbing, 2017)

$$G = U^* + pV - TS \quad (5)$$

where  $G$  is the free energy [J/mol],  $V$  is volume [ $\text{m}^3$ ],  $p$  is the pressure [Pa],  $T$  is the temperature [K],  $S$  is the entropy [J/k] and  $U^*$  is the internal energy [J]. (Ebbing, 2017)

By deriving the equation 6 and making the equilibrium equation from two different points on the curve, the Clapeyron equation can be derived. The equation for Clapeyron is the equation 6.

$$\frac{dp}{dT} = \frac{\Delta H}{T\Delta V} \quad (6)$$

where  $H$  is the enthalpy [J/mol],  $V$  is volume [ $\text{m}^3$ ],  $p$  is the pressure [Pa] and  $T$  is the temperature [K]. (Ebbing, 2017)

The freezing point of salinity water as a function of pressure is calculated with Clapeyron equation and plotted in figure 18. The pressure is between 1 bar to 16 bar and the salt content is up to 10 ‰. The salt content of the water is on average 5 ‰ to 8 ‰ and the figure 18 shows that the effect of pressure on freezing is about 0,25 °C to 0,5 °C.

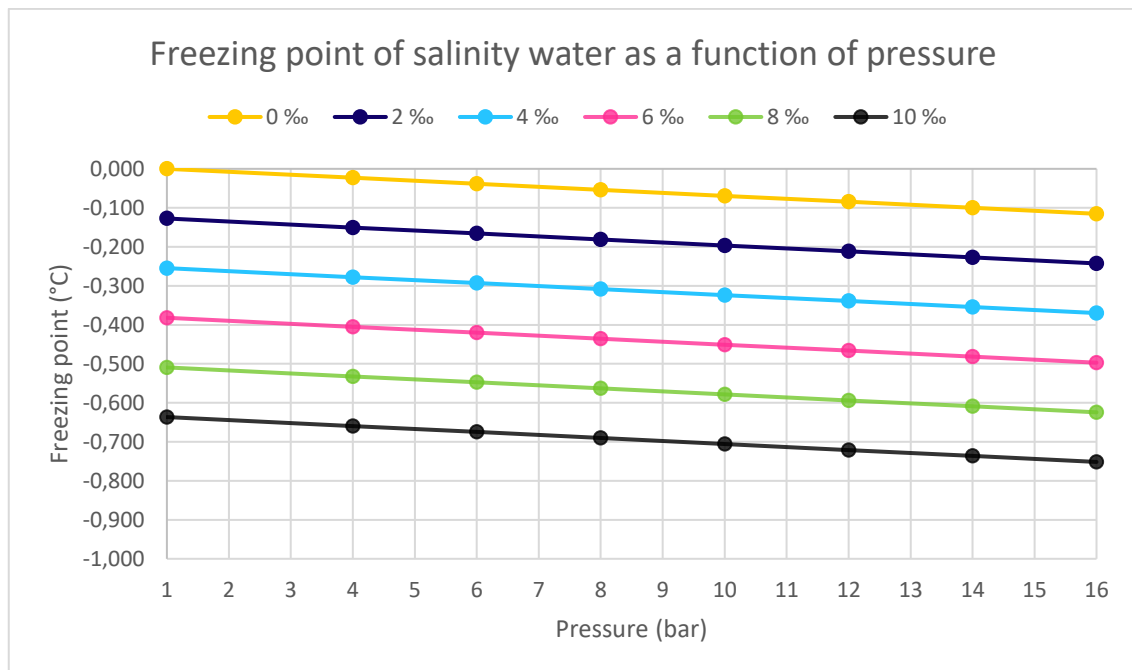


Figure 18 Freezing point of salinity water as function of pressure

### 3.4 Seawater density

The density of seawater is one of the most important quantities in physical marine research. The seawater density is affected by salinity, temperature and pressure. It can be expressed in a general form in the equation 2. The density of seawater does not vary much due the Baltic sea salinity, but the density of seawater can be determined by combining the masses of water and salt.

$$\rho = \rho(s, T, p) \quad (2)$$

where  $\rho$  is the density [ $\text{kg}/\text{m}^3$ ],  $s$  is the salinity [‰],  $T$  is the temperature [ $^{\circ}\text{C}$  or  $\text{K}$ ] and  $p$  is the pressure [ $\text{Pa}$ ]. (Myrberg et al., 2006)

The compression of seawater is approx.  $0,5 \cdot 10^{-4} \text{ bar}^{-1}$ . At a depth of 70 meters there is a pressure of about 7 bar, whereby the compression is about 0,35 %. In practical problems, local vertical changes in density are important for stability, but in the Baltic Sea the effect of pressure is not significant. Instead, the effect of pressure in the deep waters of the oceans must be considered. The effect of pressure is largest at a Landsort depth of 459 meters, increasing the density by about 0,2 %. The density of seawater in the Baltic Sea is about 1,000-1,010  $\text{kg} / \text{m}^3$ .

In the vertical distribution of seawater density, the pressure effects adiabatically. In the adiabatic process, the water particle does not change heat with the environment, but its temperature changes due to the change of pressure. As the water particle rises in the sea, the hydrostatic pressure of the surrounding water decreases, resulting decrease in density and the work required to expand the water particle consumes internal energy. In this case, the temperature of the water particle decreases. Correspondingly, deeper the density and temperature increases. This is important when researching the stability of the water body. Potential temperature refers to the temperature that a water particle is moved adiabatically to a surface without changing its salinity. The potential density is the density determined by the potential temperature. In the Baltic Sea, water is stratified, but stratification varies according to water stability, which depends on the vertical distribution of water density. The stratification is usually stable or neutral. In a stable situation, lighter water is on top of heavier water, and in a neutral situation the potential density is constant. In an unstable situation, the density of the water surface increases, it tends to sink, and light water rises. The mixing of the water continues until the stratification has become stable or neutral.

### 3.5 Thermocline and halocline

The boundary layer between two different bodies of water is called the leap layer, i.e. the clinic. In a layer, the density changes strongly over a few meters, so the change is abrupt in

nature. The temperature leap layer is called the thermocline. In the spring, after the ice melts, the sun heats the thin layer of seawater and the energy balance on the sea surface is positive, meaning the sea gets more heat than it gives up. The water then reaches the maximum density temperature (with Baltic seawater at a temperature of approx. 2-3 °C). After that, the warming surface water is lighter than the water below it. Convection ceases and a thermocline is formed between the warm surface water and the colder deeper water. The thickness of the thermocline is about 5-10 meters. The thermocline will become strong in the summer and the temperature may drop by ten degrees within a few meters. As the summer progresses, the thermocline thickens due to wind-induced mixing. The thermocline also helps the freshwater brought by the rivers to remain in the surface layer and this reinforces the density difference above and below the thermocline. It can be seen from figure 11 that in August the surface water is considerably less saline than the deeper water. At the end of August, the sea level energy balance will turn negative and the surface water will cool. As surface water cools, it becomes heavier and it sinks. The surface layer thickens, and the thermocline weakens. The heat is transferred downward by convection and the process continues as the fall goes forward. Although the maximum density temperature of the Baltic Seawater is about 2-3 °C, the temperature of the entire cover layer usually decreases to close to 0 °C due to wind-induced mixing. (Myrberg et al., 2006)

Halocline cannot be removed by convection or wind. The salinity of surface water in the Baltic Sea is generally constant. The salinity increases rapidly as you go deeper at 60-80 meters and this leap is called the halocline. Halocline isolates deep water from surface waters and impairs or completely prevents the transport of oxygen into deep water. In the Baltic Sea, oxygen is usually depleted from deep waters, after which hydrogen sulphide begins to form. In areas with low stratification (vertical ones are small), the halocline may disappear during autumn and winter storms. This can happen, for example, in the western Gulf of Finland. The halocline goes away completely, if saltwater replenishment does not regularly flow into the Gulf of Finland from the main basin of the Baltic Sea. During the history of marine research, periods of weakened or almost disappeared haloclines of various lengths have been observed in the Gulf of Finland. The most recent and best-documented period began in the early 1980s and continued for almost two decades. The reason for the weakening of the saltwater inflow was a long period without salt pulses coming from the North Sea through the Danish straits. Due to the river water pressure, the direction of the flow is mainly outward towards the North Sea. In certain special situations, the flow

direction reverses and salty water flows from the North Sea to the Baltic Sea. This phenomenon is called a salt pulse. The first condition for the creation of a salt pulse is a long-term easterly air flow, which promotes the flow of water out of the Baltic Sea. Lower-than-average river flows are also an advantage for the development of a favorable situation. As a result of these, the surface of the Baltic Sea temporarily drops below the surface of the North Sea. When the wind turns back to the west, water starts to flow towards the Baltic Sea. If this situation is combined with a strong storm from the west or southwest, a strong salt pulse can flow into the Baltic Sea. Generally, the biggest salt pulses have entered the Baltic Sea in the winter season. The last significant salt pulse arrived in the Baltic Sea in 1976, after which the cod population became abundant so that cod fishing off Helsinki became almost a popular pastime. However, the cod quickly disappeared. The Baltic Sea received its next salt pulse only in 1993. A significant amount of salty water was added only in the 21st century. (Myrberg et al., 2006)

The seawater temperature has a leap layer in the summer called the thermocline. It separates the surface layer from the much colder intermediate layer. The summer thermocline is usually formed to a depth of 10 to 20 meters. The water in the warm surface layer does not mix with the cold water below the thermocline. The water in the surface layer is evenly warm in the depth direction due to the mixing caused by the wind, but the water below the thermocline mixes only occasionally. In the fall, when the surface water cools, the thermocline disappears. Autumn storms and flow due to temperature differences, i.e. convection, confuse the water masses. In the Baltic Sea, water mixes only up to a permanent halocline.

### 3.6 Characteristics of the seafloor

In the Gulf of Finland, the Finnish coast is shallow and archipelago, with an average depth of 20-40 meters. Figure 19 shows the Gulf of Finland and the Helsinki area marked in blue. from which you can see that in the Gulf of Finland it is possible to reach depths of 80 meters, but depths of 100 meters are encountered when going towards the main basin of the Baltic Sea.



Figure 19 Depth of the Gulf of Finland (Myrberg et al., 2006)

Figures 20 and 21 show the depth curve retrieved from the retkikartta.fi service. The map shows that near Isosaari there are 50-meter depths, which is the water intake point discussed in the study. The distance is about 17 km, which is given in the initial data of the study. The study also provides a longer tunnel option, approx. 27 km and approx. 70 meters deep. It is not shown in figure 20.

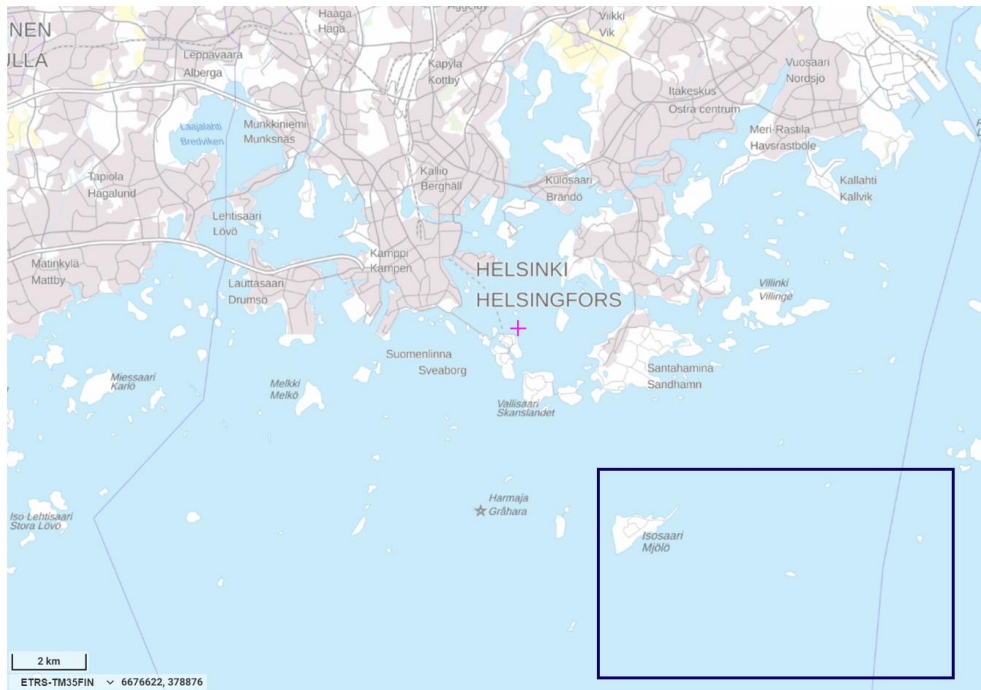


Figure 20 Depth of the Helsinki area (retkikartta.fi, 2022)

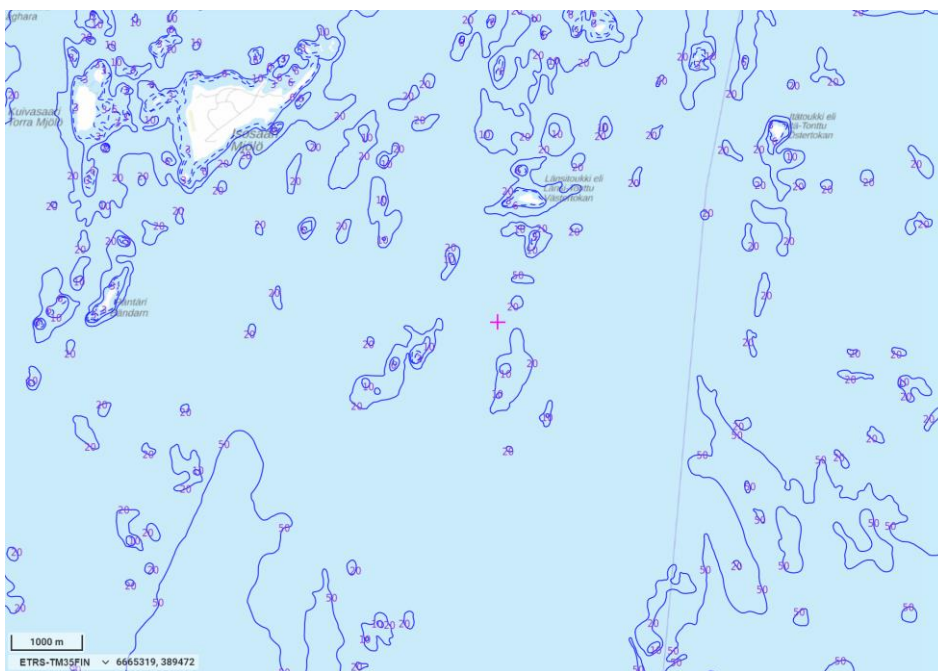


Figure 21 Depth of 50 m in the Helsinki area (retkikartta.fi, 2022)

The deposits on the bottom of the Baltic Sea vary a lot between different areas. Sediments can be divided according to the way they are formed into two, glacial and post-glacial deposits. Glacier-born sediments are deposited on the bottom or in front of the glacier. They

are moraines, glacial rock deposits such as ridges and loamy clays. Post-glacial deposits are mainly fine-grained sediments such as clay and silt. Coarse-grained sediments deposited by erosional forces also belong to this group. Figure 22 shows a typical layer arrangement from the western Gulf of Finland. (Itämeri.fi, 2017)



Figure 22 Typical seabed deposits of the Gulf of Finland (Itämeri, 2017)

These sediments are briefly introduced in this study because they affect seawater filter placement and design. If there is, for example, 10 meters of clay or silt on the seabed, placing the filters on the seabed may require modification of the bottom and/or piling.

### 3.7 Characteristics of sea surface

There is a small crustacean in the sea called sea pox, which lives as a larva in open water. The larvae are difficult to see before they attach to surfaces because they are less than a millimeter in size. When the sea pox attaches, it no longer moves but grows on the surface to become an adult. A single larva looks like a centimeter-sized calcareous formation, but usually there are a group of them. According to current knowledge, there are no other species of sea pox in the Baltic Sea. Sea pox larvae usually attach to surfaces for a few weeks

between July and August. A couple of weeks after being attached, they can be easily removed from the surfaces, for example with a pressure washer or by brushing by hand with a coarse sponge or root brush without detergents. Later removal is more difficult because after the development of the calcareous shell of the sea pox, they are firmly attached to their surface. (Vieraslajit.fi, 2012)

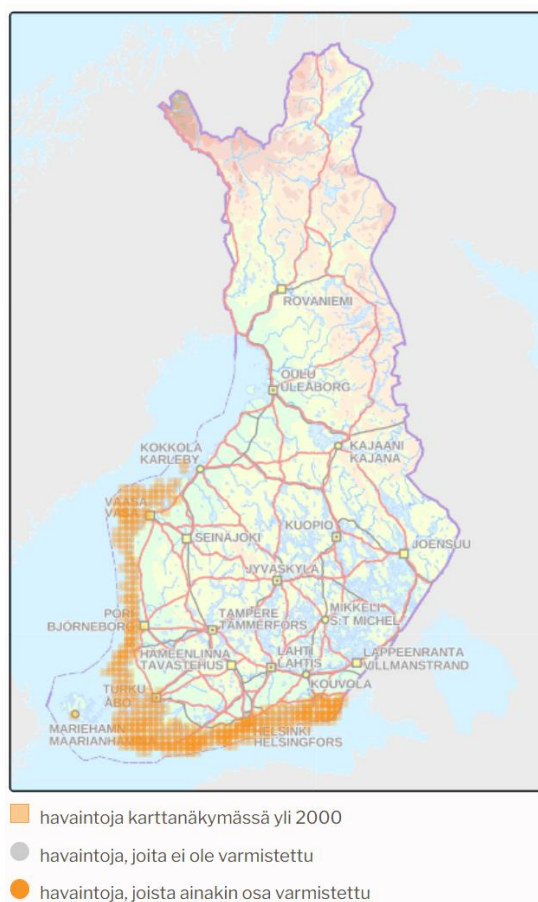


Figure 23 Sea pox in the Baltic Sea (Vieraslajit.fi, 2012)

The sea pox occurs everywhere in the Baltic Sea where the water salinity is at least 3 ‰, so it is away from the Bothnian bay. Sea pox lives on solid surfaces in groups or colonies from the water line to a depth of about 15 m, sometimes even deeper. Close to the water line, sea pox forms very dense deposits under favorable conditions. (Luontoportti, 2022) The sea pox usually attaches to surfaces in the Baltic Sea when the water temperature has exceeded 18 °C. (Myrkyttömästivesillä.fi, 2022) Ice limits the presence of sea pox near the surface, but the species can withstand low temperatures. However, constant low temperatures (5–10°C) inhibit reproduction. (Luontoportti, 2022)

As we discussed, sea pox needs the right conditions to survive. The seawater intake can be too deep, too less salt or too cold for sea pox. Although the seawater intake is at a depth of 70-50 meters, the sea pox will be a challenge because surface water is used in the summer months. In addition, sea pox larvae are less than a millimeter in size, so they can pass through the seawater intake channel. The filter/net of the seawater surface water intake channel will probably be larger than 1 mm hole size. The following sections show how these aspects affect the utilization of seawater heat in heat pump processes and how the challenges can be solved.

## 4 Fouling of heat exchangers

Fouling is a typical issue in heat exchangers that contains impurities. The heat exchanger should meet the process requirements after fouling. If possible, the heat exchanger should be designed to self-clean or that the growth rate of the fouling layer slows down and eventually stops at a certain level. Before the annual maintenance or the cleaning of the heat exchanger, the exchanger must be able to transfer heat according to process values. An extra heat transfer surface area or an extra heat exchanger can be added to help with fouling process. (Saari, 2010) However, oversizing the heat exchanger can accelerate fouling because oversizing lowers flow rates and probably accelerates fouling. If the heat transfer deteriorates, the cold current does not heat up or the hot current does not cool down sufficiently, this might require additional heating or cooling. This is not always noticed, or this is ignored if the process works anyway. Sometimes the decrease in the heat transfer coefficient is compensated by increasing the flow rates, resulting in increased pressure losses. In this case, the energy required for pumping increases exponentially. Pressure losses also increase without an increase in flow rates, as the cross-sectional area of the flow channels decreases, and the flow resistance increases. (Motiva, 2022)

## 4.1 Prevention of fouling

Heat exchangers can be prevented from getting unclean and energy efficiency can be improved by proper use, cleaning during operation and flushing of the system before commissioning. As one basic principle, it can be stated that heat exchangers should be run continuously at full power, if that is possible. In that case the flow rates remain high, which prevents fouling and deterioration of energy efficiency. If the temperature levels can be influenced, the general guideline is to keep them low.

The means of reducing fouling problems are

- the operations during use,
- the procedures during a maintenance shutdown (in practice thorough cleaning of heat exchangers) and
- heat exchanger design methods.

Mechanical filtration of the flowing medium to remove excess material is a typical mechanical cleaning method. Momentarily increasing the flow speed removes dirt, especially from points where the speed decreases locally. There are also flow direction changers that help heat exchangers stay clean. A flow direction changer is practically a valve that turns the flow in a different direction. Some of the heat exchangers can be opened and cleaned mechanically. There are ball cleaning systems for tube heat exchangers that clean the tubes mechanically. These will be reviewed later in this study.

Chemical cleaning is used when it is not possible to dismantle the heat exchanger or the dismantle takes too much time. CIP washing (cleaning in place) is a chemical cleaning method. In chemical cleaning, a cleanser solution is directed to the heat exchanger through the pump and pipeline. A cleanser solution it is circulated for the necessary time inside the heat exchanger, usually few hours.

## 4.2 Heat transfer

There are four basic variables in the calculation of heat exchangers, they are the heat transfer rate, heat transfer area, heat capacity rates and the overall heat transfer coefficient. However, this work does not provide an in-depth introduction to the sizing of the heat exchanger, only from the point of view of fouling. The equations used to calculate the heat transfer have been determined with these assumptions. The basic equation for heat transfer rate is in the equation 7.

$$q = \dot{m} c_p \Delta T \quad (7)$$

$c_p$  is the specific heat (for water 4184 J/kgK),  $\dot{m}$  is the massflow [kg/s], where  $q$  is the heat transfer rate [W],  $\Delta T$  is the temperature difference of the two fluids in the heat exchanger [K].

The heat exchanger's dimensioning uses the mean temperature difference, according to which the area of the heat exchanger is decided. The temperature difference changes continuously throughout the heat exchanger; for this reason, the selection of a mean value must be carefully done. The mean temperature difference is calculated using the equation 8a.

$$\Delta T_m = \frac{\Delta T_{in} - \Delta T_{out}}{\ln(\Delta T_{in} / \Delta T_{out})} \quad (8a)$$

where  $\Delta T_m$  [°C, K] is the mean temperature difference,  $\Delta T_{in}$  [°C, K] is the temperature difference one side and  $\Delta T_{out}$  [°C, K] is the temperature difference other side (figure 42). (Saari, 2010)

By using the mean temperature difference, the heat transfer rate can be calculated with the equation 8b.

$$q = G\Delta T_m \quad (8b)$$

where  $q$  is the heat transfer rate [W],  $\Delta T_m$  [°C, K] is the mean temperature difference and  $G$  [W/°C] is the conductance.

There are two kinds of fluid flow, laminar and turbulent flow. Laminar or turbulent conditions it can be determined using the Reynolds number and it can be calculated with equation 9. Below  $Re = 2000$  the flow is laminar and above  $Re = 3000$  the flow is turbulent. The region between  $Re = 2000$  and  $3000$  is more unclear and often referred to as the transition zone. Velocity is distributed differently in laminar and turbulent flow. In laminar flow, the velocity profile is a parabola, in which case the mean flow velocity is half of the velocity in the middle of the pipe (maximum velocity). In turbulent flow, the velocity profile is no longer a parabola but for turbulent flow the mean velocity of the fluid in the pipe is  $0,82$  x the velocity in the middle of the pipe. Even in turbulent conditions, there is a thin, slowly moving laminar layer on the surface of the pipe (usually referred to as the viscous sub-layer).

It is possible to calculate the heat transfer coefficient of the liquid flowing inside the pipe using the numbers of Reynolds (equation 9), Prandtl (equation 10) and Nusselt (equation 11).  $D$  is the hydraulic diameter of the pipe (the inside diameter if the pipe is circular).

$$Re = \frac{uD}{\nu} \quad (9)$$

where  $\nu$  is the kinematic viscosity [ $m^2/s$ ],  $D$  is the hydraulic diameter [m] and  $u$  is the mean velocity of the fluid [m/s].

$$Pr = \frac{\mu c_p}{k} \quad (10)$$

where  $\mu$  is the dynamic viscosity [Pa\*s],  $c_p$  is the specific heat [J/kgK] and  $k$  thermal conductivity [W/mK]. (Saari, 2010)

For pipe flow in the turbulent region ( $Re < 3000$ ) the Nusselt number can be calculated with equation 11. The equation often considered the most accurate is the Gnielinski correlation. (Aittomäki, 2012)

$$Nu = \frac{\left(\frac{f}{8}\right)(Re-1000)Pr}{1+12,7\left(\frac{f}{8}\right)^{\frac{1}{2}}(Pr^{\frac{2}{3}}-1)} \quad (11a)$$

$$f = (0,79 \ln(Re) - 1,64)^{-2} \quad (11b)$$

With these equations, the heat transfer coefficient for the liquid flowing in the pipe can be calculated using the equation 12.

$$h = \frac{Nu k}{d_s} \quad (12)$$

where  $h$  is the heat transfer coefficient [W/m<sup>2</sup>K],  $d_s$  is the pipe inside diameter [m] and  $k$  thermal conductivity [W/mK]. (Saari, 2010)

Determining the U-value of the total heat transfer coefficient is a key thing in the design of a heat exchanger, but often designers use an inaccurate value in the heat exchanger design, and this brings design problems. Fouling resistances must be assessed when dimensioning the heat exchanger. The determination of U is affected by the geometry of the heat exchanger, the directions of the flows and the quantities.

The overall resistance to heat flow increases as the surfaces of the heat exchanger foul. Figure 24 shows how the dirt layer affects the temperature distribution.  $T_h$  and  $T_c$  are the temperatures of the hot fluid and cold fluid and in this case, we investigate the seawater as a

hot fluid and the refrigerant as a cold fluid. Temperatures reach almost to the boundary layer in turbulent conditions, because the good mixing occurs rather than solids or slow-moving fluids. The thermal conductivity of foulants are usually lower than of metals, which have relatively high thermal conductivity. For these reasons, relatively large temperature differences are needed to conduct heat through the deposits, while the temperature difference across the metal wall is comparatively small. The fouling is also affected by flow rate, temperature, and concentration. From the literature the fouling resistance in shell and tube heat exchangers with seawater is 0,000175-0,00035  $\text{m}^2\text{K}/\text{W}$  when maximum seawater outlet temperature is 43 °C. This study deals with the Baltic Sea, which is brackish water, and it has a larger fouling resistance 0,00035-0,00053. These values assume: “For tube side, the velocity of the stream is at least 1.22 m/s for tubes of non-ferrous alloy and 1.83 m/s for tubes fabricated from carbon steel and other ferrous alloys. For shell-side flow the velocity is at least 0,61 m/s.” (Bott, 1995)

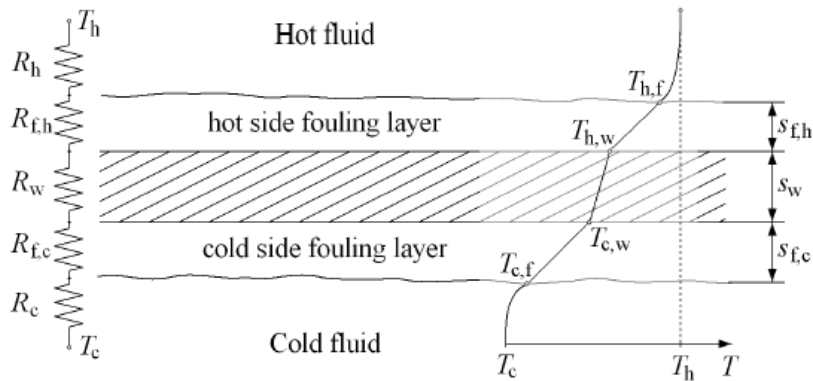


Figure 24 Effect of fouling on heat transfer (Saari, 2010)

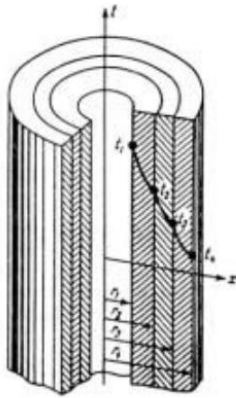


Figure 25 Multilayer pipe heat flux (Aalto University, 2019)

The increased heat transfer resistance can have two effects. When deposit thickness is notable, area of fluid flow is reduced. For the flow, the fluid velocity and the Reynolds number will increase, and the higher number of Reynolds increases the turbulence of the flow. In addition, the roughness of the pipe change which will change the turbulence particularly near the surface. Usually, the roughness is greater due fouling when turbulence of the flow increases. Greater turbulence will increase the heat transfer. (Bott, 1995)

Considering the heat transfer resistance created by the dirt or ice layer. The heat transfer rate can be shown also with the thermal resistance, without U-value or area. (Saari, 2010)

$$q = \frac{(T_h - T_c)}{R_{tot}} \quad (13)$$

where  $q$  is the heat transfer rate [W],  $T_h$  is the temperature inside the pipe [ $^{\circ}\text{C}$ , K],  $T_c$  is the temperature outside the pipe [ $^{\circ}\text{C}$ , K],  $R_{tot}$  [K/W] is the sum of surface convection resistances and the conduction resistances through the heat exchanger wall material and layers of fouling material on both sides of the surface.

Convection resistances outside  $R_c$  and inside  $R_h$  the pipe are calculated from the definition of convection resistance and area, equation 14.

$$R_{conv} = \frac{1}{hA} = \frac{1}{\pi d L h} \quad (14)$$

where the convection heat transfer coefficient  $h$  [W/m<sup>2</sup>K], the area is  $A$  [m<sup>2</sup>],  $L$  is the length [m] and the  $d$  is the diameter [m].

The wall conduction resistance can be calculated from equation 15,

$$R_w = \frac{w}{k_w A} = \frac{\ln\left(\frac{d_o}{d_i}\right)}{2\pi k_w L} \quad (15)$$

where the convection heat transfer coefficient  $h$  [W/m<sup>2</sup>K], the area is  $A$  [m<sup>2</sup>],  $w$  is wall thickness [m],  $L$  is the length [m],  $k$  is the thermal conductivity [W/mK],  $d_o$  is the outer diameter [m] and  $d_i$  is the inner diameter [m].

Fouling resistance is usually not calculated from the thickness or thermal conductivity of the fouling layer, as these are not generally known. Typical fouling resistances are available in the literature for various fluids and heat exchangers, but these are indicative only. Figure 26 shows the fouling resistances with different mediums. Fouling resistances are nearly 10 times lower in plate heat exchangers than in shell-and-tube heat exchangers. (Awad, 2011) From the literature the fouling resistance in a shell and tube heat exchangers with seawater is 0,000175-0,00035 m<sup>2</sup>K/W when maximum seawater outlet temperature is 43 °C. This study deals with the Baltic Sea, which is brackish water, and it has a larger fouling resistance 0,00035-0,00053 m<sup>2</sup>K/W (in figure 26 the rives has the same fouling resistance). (Bott, 1995)

Process Fluid	$R_f$ , (m <sup>2</sup> · K/kW)	
	PHEs	TEMA
Soft water	0.018	0.18–0.35
Cooling tower water	0.044	0.18–0.35
Seawater	0.026	0.18–0.35
River water	0.044	0.35–0.53
Lube oil	0.053	0.36
Organic solvents	0.018–0.053	0.36
Steam (oil bearing)	0.009	0.18

Figure 26 Typical fouling resistances  $R_f$  for PHEs THEs (Awad, 2011)

The fouling layer resistance then obtained from equation 16. (Saari, 2010)

$$R_f = \frac{R''_f}{A} = \frac{R''_f}{\pi dL} \quad (16)$$

where the area is  $A$  [ $m^2$ ],  $L$  is the length [ $m$ ] and the  $d$  is the diameter [ $m$ ].

From the above thermal circuit analogy and equations, we can now write  $U$  total heat transfer coefficient. (Saari, 2010)

$$\frac{1}{U_h A_h} = \frac{1}{U_c A_c} = \frac{1}{h_h A_h} + \frac{R''_{f,h}}{A_h} + R_w + \frac{R''_{f,c}}{A_c} + \frac{1}{h_c A_c} \quad (17)$$

The assumption above is that both fluids are either liquids or non-radiating gases. If one or both fluids is a gas with significant emissions or absorption of radiation due to particles, droplets or gas components, the effect of radiation heat transfer between the heat transfer surface and the gas must also be considered. The calculation of other type of heat exchangers are done according to the same principles, but the calculation changes slightly when the geometry changes.

Heat transfer depends on the properties of the refrigerant and temperature differences. Dependence is expressed by experimentally determined equations, i.e. correlations. Correlation for bubble boiling of oil-free refrigerant on the surface of a horizontal tube is presented below. This correlation is presented by Stephan and Abdelsalam, which can be represented as equation 17. The coefficient  $C_2$  can be seen in figure 27. (Aittomäki, 2012)

$$h = C_2 * (T_p - T_{sat})^{2,922} \quad (17)$$

where  $h$  is the heat transfer coefficient [ $W/m^2K$ ],  $T_p$  is the pipe surface temperature [ $^{\circ}C$ ]  $T_p$  is the refrigerant saturation temperature [ $^{\circ}C$ ] (Aittomäki, 2012)

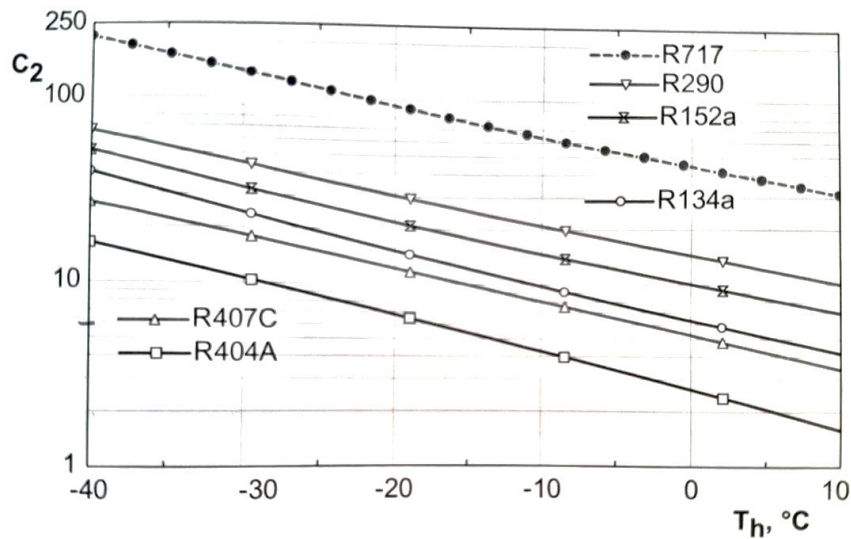


Figure 27 The coefficient  $C_2$  for the equation 17 (Aittomäki, 2012)

### 4.3 Methods of fouling

The fouling mechanisms of heat exchangers are particulate deposition, crystallization freezing, corrosion, chemical reaction, biofouling and mixed systems. (Bott, 1995) This study focuses on the fouling mechanisms relevant to the perspective of the research problem, freezing, particulate deposition and biofouling. The formation and development of fouling is affected by the properties of the medium, such as salinity, temperature and solids. Also, the heat exchanger material and construction affect fouling mechanisms.

#### 4.3.1 Freezing

The flow does not affect the freezing temperature, but it does affect the rate of heat transfer. Depending on the temperatures of the surfaces on the opposite side, the flow can either slow down or speed up freezing. When the water is flowing in a river, the water mixes between the layers, so the ice layer does not form as quickly as in the case of static water. Warmer groundwater can move to the surface. Eventually, the entire body of water cools down enough and at some point, ice blocks start to form. In this case, the entire mass of water cools

close to the freezing temperature and freezing occurs faster. If an ice layer started to form on the surface of the pipe, the water moving inside pipe would transfer its heat to the ice layer/pipe surface more efficiently (forced convection) and help prevent the ice layer from thickening, because new water is constantly replacing it. There is no critical speed after which there is an abrupt transition from fast freezing to slow freezing. So, in theory the moving water freezes faster, it's just that freezing is delayed longer, and the static water freezes sooner, not faster. (Laitinen, 2022)

When a liquid is flowing and other side of wall temperature is below the freezing point of the liquid, solidification of the liquid can appear. The solid layer of ice works as a thermal resistance and heat removal decreases from the flowing liquid. It is a similar process than a crystallisation, but mass transfer to the surface does not happen, the depositing molecules are already at the surface. (Bott, 1995)

Figure 28 shows how an ice layer is formed under static conditions when the temperature of the metal surface is below the freezing point ( $0\text{ }^{\circ}\text{C}$  with water). Sensible heat and the latent heat (phase change) are removed from the water at the liquid/solid interface. In a static conditions heat pass from the water to the cold metal surface by conduction. The ice thickness increases with the associated increased in thermal resistance. When ice thicknesses the heat transfer decreases and this will represent an exponentially decreasing rate of growth of the ice layer. Boundary between the liquid water and the solid changes, it is called transient condition. With transient condition and complex ice structure, which depend on rate of cooling, make severe problems of mathematical analysis. (Bott, 1995)

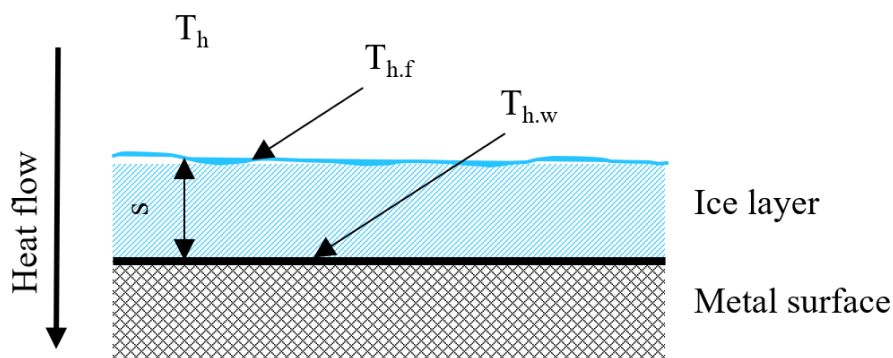


Figure 28 Ice formation at a surface below freezing point

Figure 29 shows the freezing time-temperature relationship of pure water. Supercooling occurs first, so the temperature goes below the freezing point  $T_f$  before induction of freezing (b). Pure water can be subcooled several degrees before the nucleation begins. Liquid water below the equilibrium freezing point is in a thermodynamically metastable state. It is called supercooled water and the degree of supercooling given by  $T_n - T_f$  ( $T_n$  is the nucleation temperature and  $T_f$  is the freezing temperature). The metastable state lasts until the nucleation occurs and the dendritic ice start growing in the supercooled water region (c). At the end of this dendritic ice growth process, the water temperature returns to its freezing point ( $0\text{ }^\circ\text{C}$ ) and phase change starts (d) and later the solid sensible heat is released (e). (Braga, 2012).

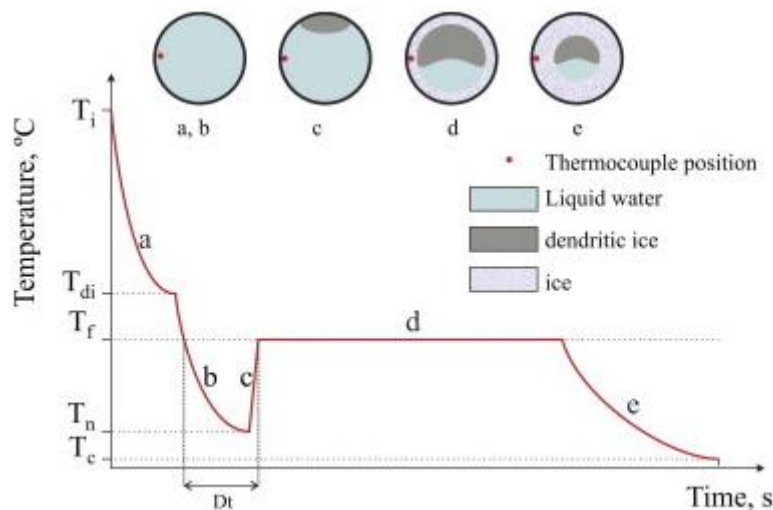


Figure 29 The process of crystallization of water (Braga, 2012)

The phase change of water is characterized by the formation of dendritic ice. Many theoretical solutions often ignore the presence of a dendritic ice zone. Theoretical predictions often do not correspond to reality closely. Gilpin (Gilpin, 1977) stated that many calculations of the time taken for a pipe to become clogged by ice are incorrect because they assume that ice grows from the walls of the pipe as a solid ring. These do not consider that dendritic ice is formed during freezing. Clogging refers to the state of the pipe when a large resistance has formed in the pipe that the water supply is completely interrupted. After the end of the dendritic growth phase, the formation of a solid ice ring begins, which begins to grow radially inward from the pipe wall. When all the water in the pipe is frozen, the pipe begins

to cool below the phase change temperature and eventually approaches the temperature of its surroundings. The pipe can break when it freezes, this usually happens when the water freezes, it causes a blockage inside the pipe, which shrinks, letting more water in between the ice and the inner surface of the pipe, freezing the pipe completely. When the pipe gets heat, the ice thermally expands, and the pressure causes the pipe to crack. (Akyurt, 2002)

Figure 30 shows a cross-section of a 150 mm pipe that was placed in the cold chamber. There is no flow in the pipe, so this represents the situation in the static case of water. The water in the pipe was supercooled just before the ice formed and pictures b-d show the growth of ice dendrites from the nucleation center near the top of the pipe. In picture e, it can be noticed that the cross-section is almost completely blocked by dendrites. This dendritic ice only took about 30 seconds in total to form. In the final stage, the temperature of the liquid returned (raised) to 0 °C. The author of the study found that dendritic ice no longer grew after the water temperature returned to zero. After this, a solid ring of ice began to form inwards, very slowly from the inner wall of the tube, photos e was taken 3 hours and photo f 18 hours after the end of dendritic ice formation. Dendritic ice can cause pipe blockage much faster than an ice ring, up to 5% of the time. When nucleation starts, it can be noticed by a rapid increase in the tube surface temperature to 0 °C. Small tubes are much more likely to be blocked by dendritic ice than large tubes. (Gilpin, 1977)

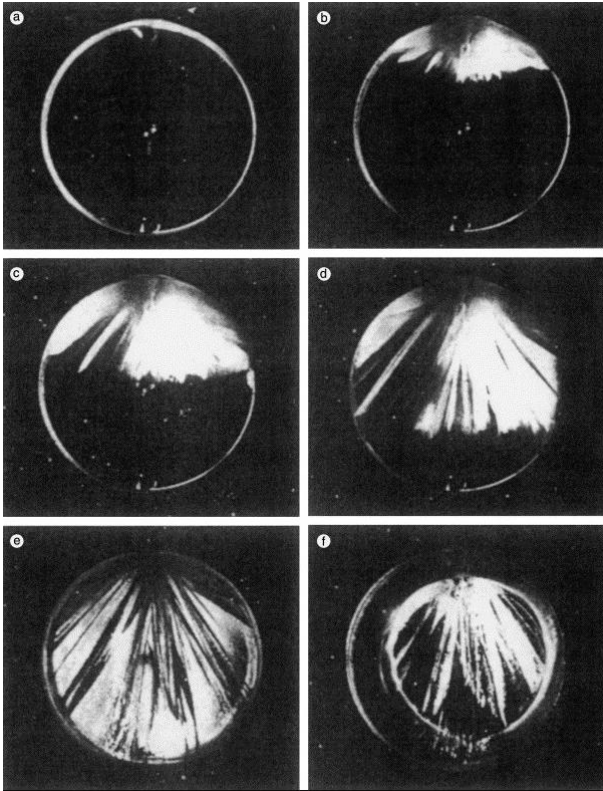


Figure 30 Formation of dendritic ice in a 150 mm pipe under static conditions (Gilpin, 1977)

The situation is further complicated by the flowing liquid. Figure 31 illustrates a situation in which the freezing flowing liquid is cooled by flowing medium on the other side of the metal wall. As a result of the temperature difference between the two liquids, there is a heat transfer that passes through the metal wall and any layer of ice or dirt. Heat transfer rate is affected by liquid type, flow resistance and dirt / ice layer. Before any ice layer is formed, the warm liquid (in this case  $\sim 2\text{ }^{\circ}\text{C}$ ) flows in contact with the metallic surface. When sensible heat is removed across the metal wall to the coolant, the temperature of the liquid in contact with the cold metal surface will eventually fall to the freezing temperature of the liquid. Freezing is possible under this condition. The heat transfer continues until the interface between the ice layer and the flowing (in this case seawater) liquid is just at the freezing point temperature. Under these conditions, steady state is reached when the ice layer remains at constant dimensions. Freezing is modified by changes in velocity as the freezing reduces the flow area and changes in surface roughness. The combination of these effects changes the heat transfer coefficient and affects the temperature distribution. The effects of the increased shear force on the surface can also affect the thickness of the solidified layer. The thickness

of the ice layer is unlikely uniform throughout the pipe because the temperature difference varies between inlet and outlet. (Bott, 1995)

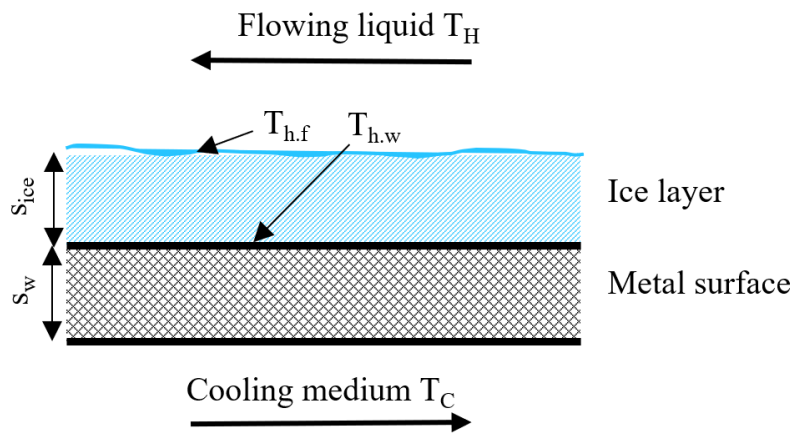


Figure 31 Freezing in a flowing system

In the case of a heat exchanger, the water passing through is constantly changing and new warm water is constantly replacing it. This slows down the freezing process. However, freezing must be taken seriously, because the heat exchanger can become blocked, for example due to dirt, in which case the flow can stop, for example, in one of the heat exchanger pipes. The previously mentioned dendritic ice begins to form in the pipe, followed by an ice layer and finally an ice plug forms in the pipe.

#### 4.3.2 Particulate fouling

The most common type of fouling in heat exchangers is particulate fouling. The particles form deposits on the heat transfer surfaces and they weaken the heat transfer. Typically, the particles are water-insoluble particles such as sand, silt or sludge.

Particle fouling can be understood as a process where a particle travels near the surface, attaches to the surface and possibly later detaches from the surface. Particles can arrive on the surface in two ways, either due to gravity or the particles come to the heat transfer surface along with the moving fluid. Deposition caused by gravity occurs in a static situation. However, in this study, a flowing fluid is studied. First, the particle travels to the surface by

one or more mechanisms. The size of the particle determines the mechanism, very small particles are prone to brownian diffusion and eddy diffusion and larger particles move due to their mass due to momentum forces. When a liquid has a certain concentration gradient, the liquid tends to move to reduce the concentration gradient. The process is known as mass transfer. In laminar flow, mass transfer occurs as a result of random motion of molecules, brownian motion. The situation is different in turbulent flow. Under turbulent conditions, eddy diffusion superimposes Brownian motion. Eddy diffusion is caused by the random physical movement of particles of fluid brought about by the turbulent conditions. A particle arriving at the surface must adhere to the surface in order to be part of the dirt layer. (Bott, 1995) When small particles and turbulent flow are put together, the fouling mechanism would be eddy diffusion. It must be remembered that even under turbulent flow conditions there is a laminar sublayer of slow-moving fluid next to the wall. Transport of material across this "boundary layer" is usually only possible through brownian or molecular motion.

If the mixture component A is diffusing through a fluid B towards a surface. Diffusion is at right angles to the general flow of fluid B, and by Fick's Law [Fick 1855].

$$N_A = -P_{AB} \frac{dc_A}{dx} \quad (18)$$

where  $c_A$  is the concentration of A at a distance  $x$  from the surface [ $\text{mol}/\text{m}^3$ ],  $N_A$  is the rate of diffusion of molecules of A [ $\text{mol m}^{-2} \text{s}^{-1}$ ] and  $P_{AB}$  is the "diffusivity" of A through B [ $\text{m}^2\text{s}^{-1}$ ]

The diffusion of A into B will depend not only on the physical properties components but also the prevailing fluid flow conditions. Since the flow is turbulent, the diffusion of A in B is increased by eddy diffusion. Under these conditions, equation 18 becomes equation 19.

$$N_A = -(D_{AB} + E_D) \frac{dc_A}{dx} \quad (19)$$

where  $E_D$  is the eddy diffusion [ $\text{m}^2\text{s}^{-1}$ ]

In general, for turbulent flow  $E_D \gg D_{AB}$  and the latter can often be neglected in the assessment of mass transfer.

The amount of seawater solids  $0,4 \mu\text{m}$  (NPC) is about 1-4 mg/l, depending on the sampling depth. (Helen internal documents, 2022) From figure 32 can be seen that with particles of size  $0,4 \mu\text{m}$ , mass transfer to the surface occurs the least when the speed is about 2 m/s. (Bott, 1995)

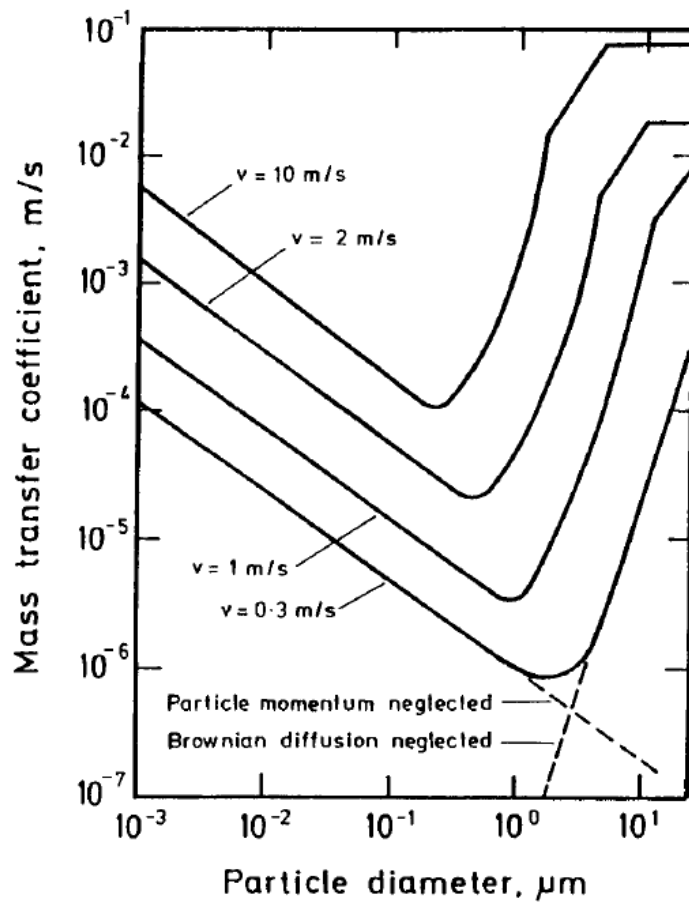


Figure 32 Effect of particle on deposition mass transfer (Bott, 1995)

#### 4.3.3 Biofouling

Biological fouling means the attachment and growth of various macro- and micro-organisms on heat transfer surfaces. Microorganisms also include algae, yeasts, fungi, moldy bacteria, and macro-organisms include mussels, flagellates and vegetation. In practice, biological fouling appears on the heat transfer surface as a biofilm that is tough and sticky. The most

typical places where biological fouling occurs are heat exchangers where natural waters are used for cooling. (Motiva)

Microfouling occurs quickly when the surface of the heat exchanger is in contact with seawater. Bacteria colonize a surface within hours and form a biofilm, which is a combination of attached cells commonly called slime. This biofilm slime layer can grow to a thickness of 500  $\mu\text{m}$ . Macrofouling includes soft and hard fouling that grows microfouling slime. Soft macrofouling includes algae and invertebrates such as sponges. Hard macrofouling is caused by invertebrates such as mussels and tube worms. The specific organisms that develop in a fouling depend on water chemistry, geographic location, season, and factors such as predation. Macrofouling is a dynamic process, and it can achieve a considerable biofouling thickness on concrete or metal surfaces. Over long periods of time, fouling accumulates in several layers and leads to a significant reduction in the available flow area. It increases the plant's flow resistance and pumping costs. In figure 33 can see the different stages of biofouling. (Brandt, 2017)

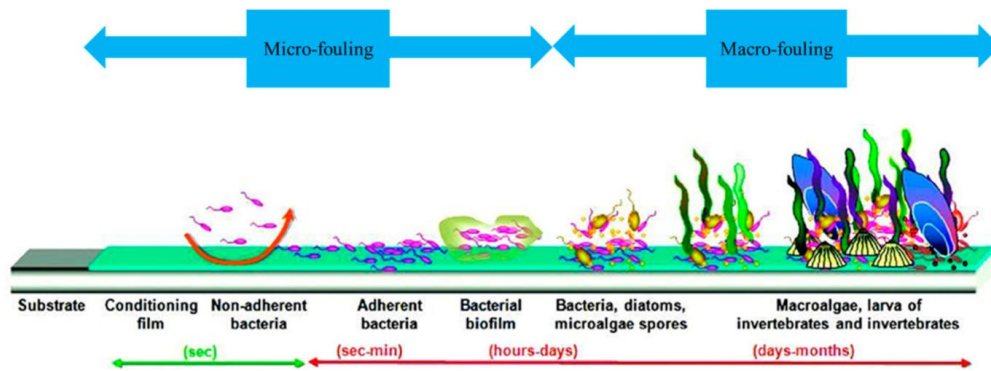


Figure 33 Biofouling formation (Hayek, 2021)

A typical biofilm growth curve for constant speed conditions is shown in figure 34. There are three areas. The first is the initial stage, when colonization takes place. The second phase includes a period of exponential growth until a third more or less stable state is reached. The thickness of the biofilm at the plateau may vary from a few micrometres to several millimetres depending on the prevailing conditions, particularly the velocity and nutrient availability. (Bott, 1995)

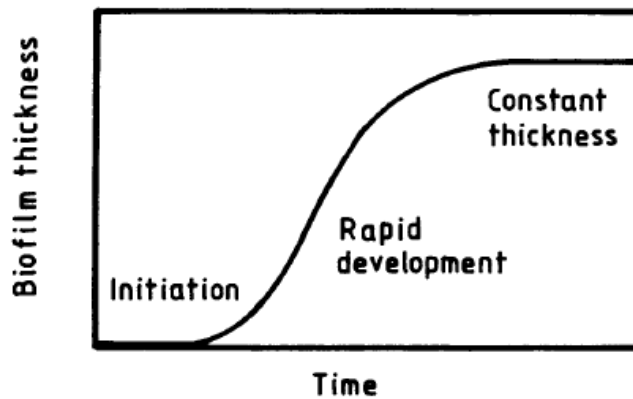


Figure 34 An idealised growth curve for a biofilm on a surface (Bott, 1995)

Figure 35 shows an example of how speed can affect biofilms. Here the Reynolds number is 12,200 and it can be seen that the speed affects the thickness of the biofilm. According to this, the biofilm gets the thickest value at speeds of 0,26-0,9 m/s. When the speed is 2 m/s, it is noticed that the biofilm no longer thickens at the same rate. This may be due to flow shear forces. This depicts the growth of *Pseudomonas fluorescens* on an aluminium surface through which water containing nutrients flowed. *Pseudomonas fluorescens* was chosen as the test organism because it is a slime-forming bacterium that represents the micro-organisms found in cooling water. With lower speeds the biofilm thickens faster than at higher speeds. It is often said a "rule of thumb" that in order to minimize biological fouling, the flow velocity should be kept above 1 m/s in steam condensers. When the speed increases, although higher turbulence increases the mass transfer of nutrients, the shearing forces also increase and at higher speeds it is difficult for a thick biofilm to remain on the surface. Even at a relatively low speed, it is possible for biofilm areas to detach from the surface. (Bott, 1995)

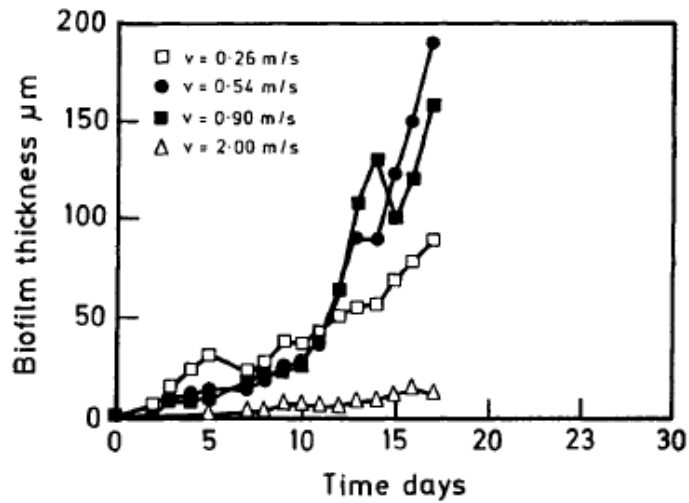


Figure 35 The development of biofilm with time at a Reynolds number of 12,200 and at different velocities (Bott, 1995)

Figure 36 show how the oxygen concentration fell at the metal-biofilm interface as the biofilm developed. (Bott, 1995) Microbiological corrosion is electrochemical corrosion acting between the biofilm and the pipe, which is controlled by the action of microbes. Microbes affect corrosion by producing corrosive compounds, breaking down the protective layer of the pipe, influencing the progress of cathode and anode reactions and creating concentration differences on the surface of the pipe. Sometimes in cold seawater, microbial corrosion can be more significant than chloride corrosion. (Outokumpu, 2009)

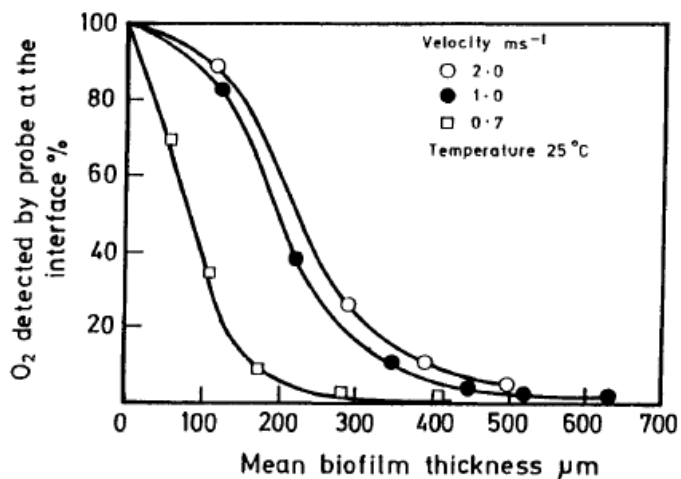


Figure 36 The change in oxygen concentration through a growing biofilm (Bott, 1995)

## 5 Case: Utilization of cold seawater in district heating production

The case deals with the utilization of seawater in district heating production. The seawater system, which is estimated to be 17 km - 27 km long seawater intake tunnel and 9 km long discharge tunnel. (Helen, 2022) This study does not take a position on tunnel drilling but deals more with the seawater heat pump section and the challenges of seawater when seawater is brought to the heat pump plant.

### 5.1 Evaporator types

This section compares different heat exchangers that could be suitable as evaporators for large size heat pumps. The evaporator medium is seawater and refrigerant. The produced heat by means of compression of the refrigerant is transferred through the heat exchanger (condenser) directly to the district heating network. The cooled down refrigerant passes through the heat exchanger (evaporator), where excess heat from the seawater is transferred into the refrigerant.

The freezing point of seawater is  $-0,3\text{ °C} \dots -0,5\text{ °C}$  depending on the salinity and pressure (in this case, varies according to the place of water intake), when the salinity and the pressure decrease, the risk of freezing increases. Avoiding the risk of freezing by reducing  $dT$  linearly increases the surface area of the evaporator and increases the amount of refrigerant charge required. Freezing occurs only in the evaporator, unless the ambient temperature of the process tubes is below the freezing point of the seawater.

One heat pump supplier keeps a margin of 0,7 Kelvin towards the water freezing point. During operation they control the freezing protection via compressor speed control and therefore an accurate control of the refrigerant evaporation pressure by low temperature seawater temperature conditions. By very low seawater temperature the evaporator is limited by the max possible or designed seawater flow. An oversized evaporator is possible but it makes the heat pump unit more expensive and higher electrical consumption for the seawater feed pump. In a direct evaporator connection where seawater enters the evaporator without

an intermediate circuit, the low seawater temperature requires a very even distribution of water on the evaporator. (Helen Oy internal document, 2022)

During operation there will be no freezing, because the water is constantly moving, and the water is over freezing point and there is a constant supply of new energy. The main risk is if the seawater stops moving for reasons such as, pump failure or valve failure. This would cause a zero-water flow through the heat exchanger. The delay time between seawater flow stopping and begin of freezing (risk) depends on many factor, evaporator heat exchanger design, minimum seawater outlet temperature, salinity and seawater flow system. It can't be generalised for all the systems and must be calculated and designed for case by case situations. The delay time in worst case conditions are in the order of some tens of seconds, therefore the evaporator must be designed, integrated and operated with a fast enough. (Helen Oy internal document, 2022)

#### 5.1.1 Shell and tube heat exchanger

The Shell-and-tube heat exchangers are available technology and used in industrial size heat pumps. Although plate heat exchangers are generally smaller, lighter and cheaper, shell-and-tube heat exchangers have held their ground in industry. The tube heat exchanger consists of a bundle of tubes that is attached inside a cylindrical shell. Figure 37 shows the flow patterns and the construction of the heat exchanger. There are many different variations of structures for shell-and-tube heat exchangers. Several structures from different manufacturers follow the standard known by the TEMA abbreviation, supplementing country-specific standards. In the case of a seawater heat pump, seawater would flow inside the pipes and refrigerant outside the pipes. When the tubes are immersed in the refrigerant

liquid, it is a wet tube evaporator. If the refrigerant flows in the pipes, it is a dry tube evaporator. (Aittomäki, 2012)

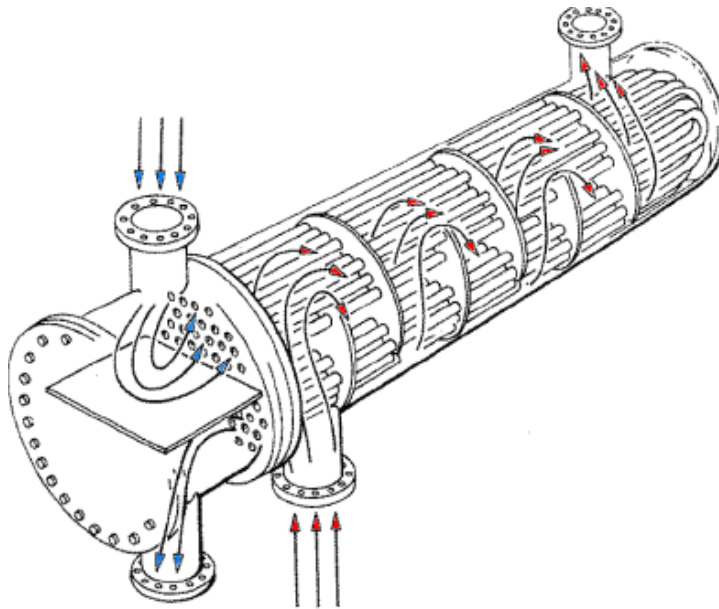


Figure 37 Shell and tube heat exchangers (Saari, 2010)

In a wet evaporator, when the refrigerant is on the shell side, the shell must be pressure resistant. It is possible to manufacture the tube heat exchanger as a very pressure-resistant structure, even in a large size. In this case, the seawater flows in the pipes, where the flow rate is limited by erosion corrosion and pressure loss. The surface level of the refrigerant must be kept constant and the liquid droplets are separated at the top of the evaporator or in a separate droplet separator, because liquid refrigerant must not reach the compressor. In a pipe heat exchanger, the heat transfer can be improved with flared pipes, figure 38. A common one is a low-ribbed tube, which improves heat transfer by up to 50-100% compared to a smooth tube. (Aittomäki, 2012)

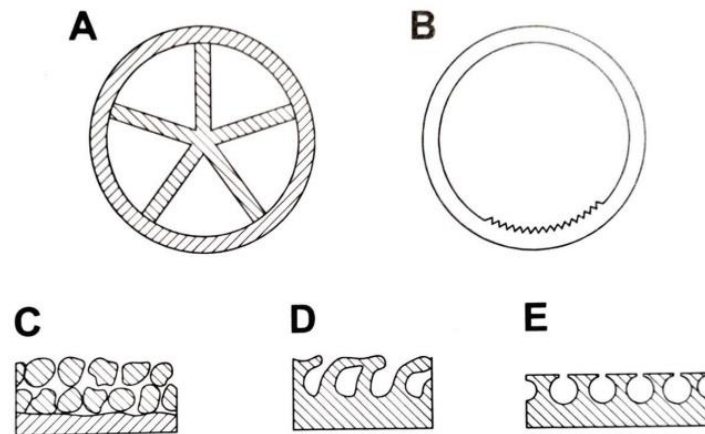


Figure 38 Surface structures for evaporator tubes to improve heat transfer (Aittomäki, 2012)

The shell-and-tube heat exchanger enables reasonably easy cleaning. The most contaminated liquid should be placed on the side of the pipe so that it is easily accessible for mechanical cleaning. But the refrigerant can also be on the shell side if contamination is not taken into account. Straight pipes should be used instead of U-pipes to make cleaning easier. This makes the evaporator longer and it does not fit everywhere due to space requirements. An automatic cleaning system, Taprogge, is available for the tube heat exchanger (more on this in section 5.2.1.3). If fouling is also a concern on the shell side, the pipe placement should be either  $45^\circ$  or  $90^\circ$  square and there should be at least 6-7 mm clearance between the pipes, so that the cleaning channels remain for mechanical cleaning. Fouling is not a problem on the refrigerant side, so there is no need to think about cleaning methods on the shell side.

### 5.1.2 Falling film heat exchanger

A falling film evaporator is designed to cool water close to its freezing point. In the falling film evaporator, the water is pumped into the distribution manifold, so that the water is evenly distributed vertically on the panels. Water flows as a thin film on the surface of the panels. In order to avoid freezing on the panels, the evaporator pressure must be adjusted. The system is open, so it is possible to clean it, mechanically, even while the machine is in use. When approaching the freezing point, the risk of ice formation increases, and the falling film evaporator has been used to reduce these risks. A falling film evaporator is not as

sensitive to ice formation as, for example, a tube heat exchanger. If ice forms on the panels for a few minutes, it will not result in mechanical destruction, it will only reduce the performance of the evaporator. The ice melts automatically when the internal temperature of the panels has risen to normal operating values. (Heat transfer technology, 2022)

With a Falling film evaporator, the flow distribution might be challenging to implement on heat exchanger surfaces and it also requires refrigerant flow control. Falling film evaporators also have disadvantages. An automatic cleaning system is not available for falling film evaporators. Falling film evaporators also take up much more space than, for example, plate heat exchangers. With seawater, the evaporator must be made of corrosion-resistant material, and the material costs are then higher. In the figure 39 is a falling evaporator.



*Figure 39 Falling film evaporator (Omt-triaca, 2022)*

### 5.1.3 Diffusion bonded heat exchangers

Figure 40 shows the diffusion bonded heat exchanger. The diffusion bonded heat exchanger withstands high pressure and temperature. It has lower volume, weight and structural support

requirements. The diffusion bonded heat exchanger can operate in temperatures ranging from cryogenic to 900 °C and pressures up to 1,000 bar. Photo-chemically etched fluid channels enable an exceptionally high heat transfer rate, which enables compact design. A diffusion bonded evaporator takes up much less space than a falling film evaporator, up to 85% less, according to the manufacturer Heatric. (Heatric, 2022) In the channels of the diffusion bonded evaporator, water goes in every other row and refrigerant in every other row, so it works like plate heat exchanger, but it has channels.



*Figure 40 Diffusion bonded heat exchanger (Heatric, 2022)*

In this process, the plates are joined to the stack by high pressure and temperature, without melting or deformation the material. The shape and size of the flow channels remain the same during the manufacturing process. The interface area between the two metal flow plates is bonded together as the atoms intertwine, allowing for an accurate structure of the flow channels within the block. In the figure 41 can be seen the interface of two metal plates, as we can see, the plates are bonded together carefully, and the interface is not seen. The plates form a metal block and it is possible to weld these steel blocks together to create a larger heat exchanger. (Heatric, 2022)



Figure 41 Grain pattern at a diffusion bonded joint (Heatric, 2018)

Ultra-high-pressure cleaning uses a diffusion bonded heat exchanger. In UHP cleaning, the high-pressure water is sprayed on fouled areas, and no chemicals are used in this cleaning method. The heat pump requires an interruption of operation and opening the end of the heat exchanger. (Heatric, 2018) Diffusion bonded heat exchangers are resistant to freezing. (VPE, 2022)

#### 5.1.4 Plate and shell heat exchanger

A plate and shell heat exchanger consist of plates stacked on top of each other with a suitable pattern pressed into them. The plates are connected to each other either by sealing, soldering or welding. The soldered or welded structure can only be cleaned chemically, and it is possible to open the sealed one. Refrigerant goes in every other gap and the fluid to be cooled in every other gap. The power can be increased by adding plates, which increases the surface area. The plate heat exchanger is more compact in size than the tube heat exchanger. A plate heat exchanger resists freezing better than a tube heat exchanger, the heat exchanger can be dimensioned close to the freezing point. (Aittomäki, 2012)

One type of plate evaporator is a shell and plate heat exchanger built inside a steel shell. The plates are welded together in pairs. One flow passes between the plates and the other inside the plates. The structure can also be made resistant to high pressure, e.g. suitable for carbon dioxide. This heat exchanger is heavier due to the thick shell, compared to soldered or

welded plate packages. (Aittomäki, 2012) Figure 42 shows an example of Vahterus plate and shell heat exchanger.

These heat exchangers have not yet been widely used in heat exchangers of industrial size, and seawater causes high material requirements. For example, a Vahterus type plate and shell heat exchanger made of titanium may still be difficult to find, but this plate heat exchanger has great potential and may be a solution for many heat pump assemblies in the future.

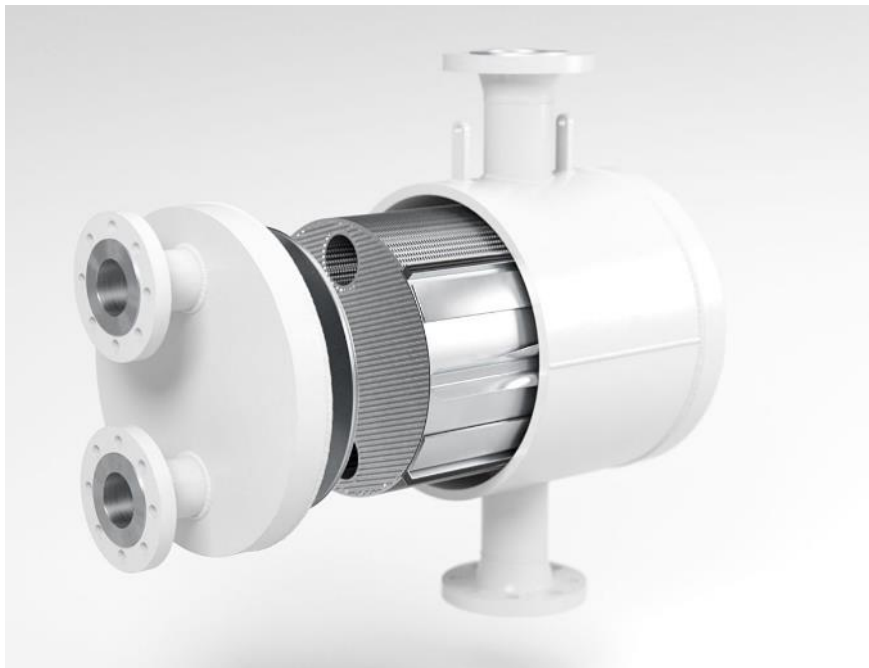


*Figure 42 Plate and shell heat exchanger (Vahterus, 2022)*

## 5.2 Evaporator the Degree of approach

The Degree of approach refers to the approach temperature, which is the difference between the required outlet temperature of the process fluid and the temperature at which utility fluid is available in the inlet. In this case, the intention is to utilize the heat of the seawater, without causing freezing in the heat exchanger. So here the degree of approach is the temperature difference between the outgoing seawater and the refrigerant. It is possible to get the degree of approach to 0,5 °C, often it is closer to 3 °. In fact, 0,5 °C is a very efficient heat exchanger.

Because seawater is an unclean liquid, it makes the degree of approach even more difficult to achieve. The figure 43 shows evaporator temperature profile and the figure 44 illustrates the evaporator flows. The temperature profile is without considering any pressure drops effect and refrigerant superheating/subcooling. The refrigerant side is isothermal because the refrigerant phase change and the seawater temperature is kept above the freezing point.

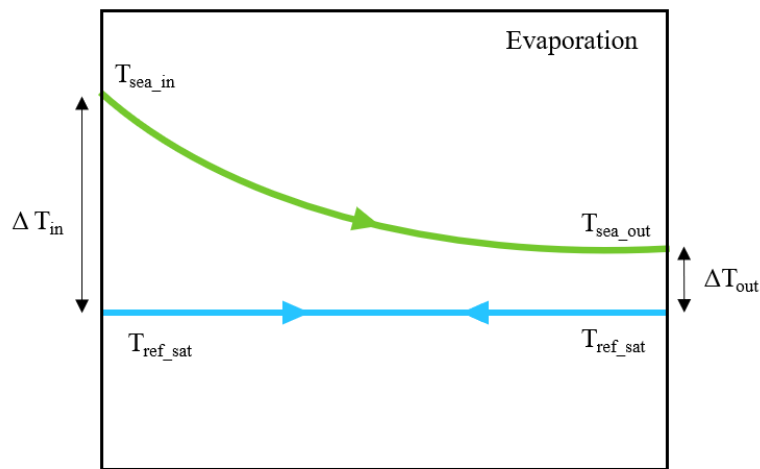


Figure 43 Evaporation temperature profile

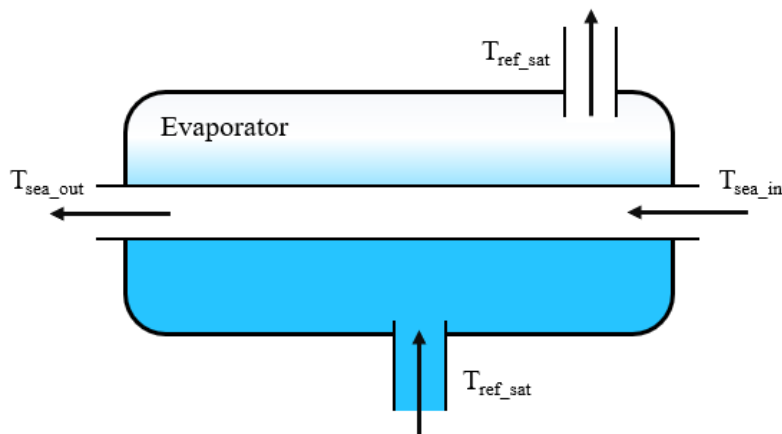


Figure 44 Evaporator flows

Figure 45 shows the seawater outlet temperature, if the temperature difference of the seawater outlet and the refrigerant is 0,5 K and it is assumed that the Baltic Sea freezes at -0,3 °C and water is taken from 50 meters depth with salinity 5 ‰ (see the section 3.3, figure 11). Then it would be possible to lower the seawater outlet temperature to 0,2 °C. However, the situation cannot be brought this close to the freezing point of seawater, it would be too risky. Figure 46 also includes a tolerance of 0,5 K for the freezing point, which was determined in accordance with the safety tolerances of one heat pump supplier. (Helen internal documents, 2022) In this case, the seawater temperature could be at least 0,7 °C. However, it should be noted that the surfaces of the evaporator pipes must not go below the freezing point, so that ice does not start to form. This is calculated in section 5.2.1.

<b>Theoretical minimum seawater temperature (salinity 5 ‰)</b>	
$T_{\text{sea\_in}}$	2,0
$T_{\text{sea\_out}}$	0,2
$\Delta T_{\text{in}}$	2,3
$\Delta T_{\text{out}}$	0,5
$T_{\text{ref\_sat}}$ (seawater freezing temperature)	-0,3
$\Delta T_{\text{m}}$	1,2

Figure 45 Theoretical minimum seawater temperature

<b>Minimum seawater temperature with safety tolerance (salinity 5 ‰)</b>	
$T_{\text{sea\_in}}$	2,0
$T_{\text{sea\_freezing temperature}}$	-0,3
$\Delta T_{\text{tolerance to avoid freezing}}$	0,5
$\Delta T_{\text{in}}$	1,8
$\Delta T_{\text{out}}$	0,5
$T_{\text{ref\_sat}}$	0,2
$T_{\text{sea\_out}}$	0,7
$\Delta T_{\text{m}}$	1,0

Figure 46 Minimum seawater temperature with safety tolerance

If the water is taken from the surface, its salinity is 2-6‰, depending on whether the water is taken from the shore or the open sea. The freezing point drops only a little, but even tenths

of a degree matter. When the salinity is 2 ‰, the minimum seawater outlet temperature is 0,32-0,82 °C, depending on the safety tolerance. In figures 47 and 48, the temperatures of 2 ‰ seawater have been calculated.

<b>Theoretical minimum seawater temperature (salinity 2 ‰)</b>	
$T_{\text{sea\_in}}$	2,0
$T_{\text{sea\_out}}$	0,32
$\Delta T_{\text{in}}$	2,2
$\Delta T_{\text{out}}$	0,5
$T_{\text{ref\_sat}}$ (seawater freezing temperature)	-0,18
$\Delta T_{\text{m}}$	1,14

Figure 47 Theoretical minimum seawater temperature

<b>Minimum seawater temperature with safety tolerance (salinity 2 ‰)</b>	
$T_{\text{sea\_in}}$	2,0
$T_{\text{sea\_freezing temperature}}$	-0,18
$\Delta T_{\text{tolerance to avoid freezing}}$	0,5
$\Delta T_{\text{in}}$	1,7
$\Delta T_{\text{out}}$	0,5
$T_{\text{ref\_sat}}$	0,32
$T_{\text{sea\_out}}$	0,82
$\Delta T_{\text{m}}$	0,97

Figure 48 Minimum seawater temperature with safety tolerance

As mentioned earlier, as the salt concentration increases, the freezing point decreases. However, it must be noted that the properties of seawater vary depending on the season, so seawater cannot be too close to the freezing point without a safety tolerance. The salinity of the water also varies depending on whether the water is taken from the bottom or the surface, and it is the Baltic Sea, which is brackish water and not an ocean.

### 5.2.1 Tube wall temperature and ice layer

The temperature of the inner wall of the evaporator tube or the ice layer surface temperature is calculated using the equations of the section heat transfer 4.2. In the calculation, it is assumed that the pipe material of the evaporator is titanium, the pipe inner diameter is 19

mm, the pipe wall thickness is 1 mm, there are 1770 pipes in total and the seawater volume flow 1717 m<sup>3</sup>/h. The calculation has been made for seawater outlet temperature of - 0,29 °C, which is just below the seawater freezing temperature with 5 ‰ salinity. In the calculation, the temperature of the refrigerant is lowered from -0,6 degrees to -4 degrees and it is determined under what conditions the temperature of the ice surface was brought close to the freezing temperature. When the surface temperature of the ice is just below the freezing point, it is assumed no more ice is formed. In the calculations, it is assumed that there is only one pipe, inside which seawater flows and outside the pipe refrigerant pool boils.

Fouling factor was not taken into account in this calculation, because it would only improve the final result of the calculation. When the evaporator is clean, even then we don't want to freeze to occur, because the dirt layer acts as an insulator. However, we are dealing with a clean surface here. Dirt prevents heat transfer, so the suction pressure of the heat pump must be increased in order to transfer the same power due to the weakening of heat transfer. If the power is kept the same and the suction pressure of the evaporator is increased, fouling can even increase the risk of freezing.

The heat transfer coefficient of the refrigerant changes continuously as the water temperature decreases, and the correlation is uncertain with small temperature differences. In any case, as the difference between the pipe surface temperature and the refrigerant saturation temperature decreases, the heat transfer deteriorates quickly. The temperature difference with 2 °C seawater may be too small for bubbling to start with smooth-surfaced pipes, the formation of bubbles can be facilitated by different surface structures and geometry of the pipes. The study analyzed the cooling of one pipe and more accurate estimates also require better correlation equations that take into account the effect of bundles of pipes. In addition, the use of ribbed pipes should be considered in the design of the evaporator, because the temperature difference between seawater and the refrigerant is low and the heat transfer on the water side is better than on the refrigerant side. (Aittomäki, 2022)

Applying the section 4.2, the equations can be written as,

$$RS = \frac{1}{\pi * d_j * h_v} + \frac{\ln\left(\frac{d_s}{d_j}\right)}{2 * \pi * k_j} + \frac{\ln\left(\frac{d_u}{d_s}\right)}{2 * \pi * k_p} \quad (20)$$

where the convection heat transfer coefficient of seawater is  $h_v$  [W/m<sup>2</sup>K],  $k_j$  is the thermal conductivity of ice [W/mK] and  $k_p$  pipe [W/mK],  $d$  is the diameter (see figure 49) and  $R_s$  is the resistance from the seawater to the outer surface of the pipe [1/(W/mK)].

$$Ru = \frac{1}{\pi * d_u * h_k} \quad (21)$$

where the convection heat transfer coefficient of sea refrigerant is  $h_v$  [W/m<sup>2</sup>K],  $d$  is the diameter (see figure 49) and  $Ru$  is the resistance from the outer surface of the pipe to the refrigerant [1/(W/mK)].

We can write a balance, the resistance from the seawater to the outer surface of the pipe, which is the same as the resistance from the outer surface of the pipe to the refrigerant.

$$\frac{T_v - T_k}{R_s} = \frac{T_k - T_{sat}}{R_u} \quad (22)$$

where  $T$  is the temperature (see figure 49) [°C, K].

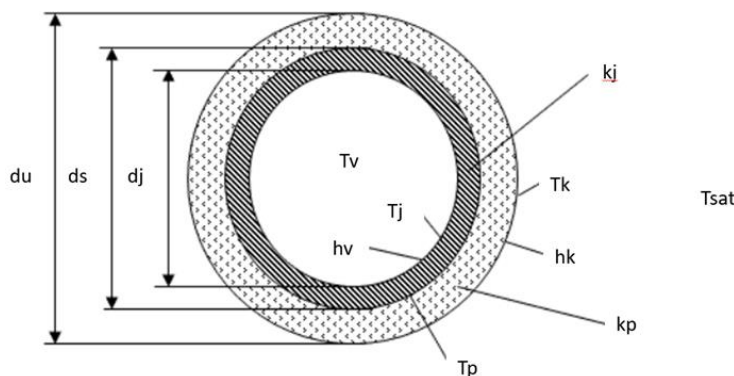


Figure 49 Explanations for equations 20, 21 and 22

Table 1 shows the surface temperature of the inside of the pipe/ice layer and the thickness of the ice layer at different refrigerant saturation temperatures and seawater outlet temperatures.

As mentioned earlier, the correlation used in the calculations is inaccurate at low temperatures and does not take into account bundled pipes. However, the figures are indicative, and it can be noticed that an ice layer starts to form when the temperature of the refrigerant drops below -1 degree and the outlet temperature of the seawater is almost at the freezing point temperature.

T_sat (°C)	T_ice/T_pipe surface (°C)	T seawater out (°C)	ice layer (m)
-4,0	-0,2983	-0,29	0,007
-3,0	-0,3019	-0,29	0,005
-2,0	-0,3015	-0,29	0,001
-1,0	-0,2912	-0,29	0
-0,6	-0,2905	-0,29	0
-0,6	-0,0010	0,00	0
-0,6	0,1973	0,20	0
-0,6	0,3960	0,40	0
-0,6	0,5940	0,60	0
-0,6	0,7907	0,80	0
-1,0	0,6798	0,80	0
-2,0	0,6131	0,80	0
-3,0	0,5463	0,80	0
-4,0	0,4795	0,80	0

Table 1 Tube wall temperatures and ice layer

### 5.2.2 Effect of seawater temperature on power

The seawater inlet temperature directly affects the district heating power. Because of the small temperature differences, seawater must be pumped in large quantities (approx. 160,000 m<sup>3</sup>/h) and for this reason the pumping power takes a lot of megawatts electricity (approx. 24 MW). Since the pumping costs are so high, with a small dT it is not necessarily worth using heat pumps. Then it is more efficiency to produce energy in another way. In this figure 50, a rough examination has been made of how the inlet temperature of seawater affects the output of district heating. Only the electricity used by heat pump compressors and by seawater pumps are considered. When the plants' energy consumption is greater than the

available district heating power, it makes more sense to produce the energy for example directly with electricity.

The changes in seawater temperatures are within 2 degrees, so it has been assumed that the COP is a constant 2.6. Also, the need for seawater pumping would be lower when  $dT$  is greater than needed, but the table assumes that 24 MW is constantly used for seawater pumping.

The figure shows that the district heating output is greater than the electricity consumption at a seawater temperature of 0,85 °C. Although it has been stated in previous sections that it is possible to reach 0,7 °C with a safety tolerance and close to zero degrees without safety tolerances, with 0,85 °C seawater, more district heating can be produced than the plant consumes electricity.

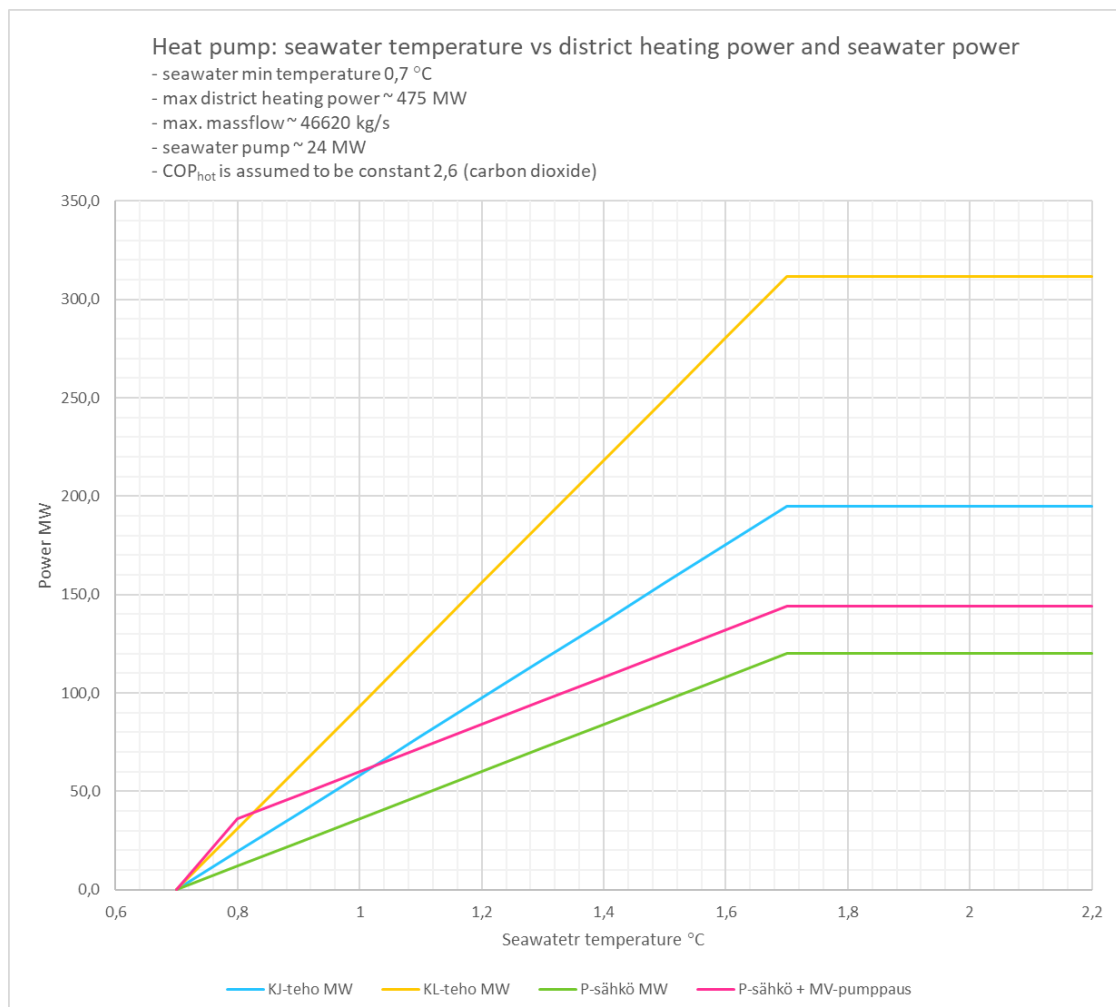


Figure 50 Seawater temperature vs district heating power

### 5.3 Filters

There are many different filtration methods for water and the choice of filter depends on the need for cleanliness. There are coarse filters, fine filters, self-cleaning filters and passive filters. Generally, a seawater system has, for example, coarse filtration and then fine filtration.

In this case, coarse filtration is possible in the open sea and its purpose would primarily be to prevent fish from entering the system, so the filtration implemented in a heat pump plant can be a self-cleaning filter with a finer degree of filtration. Relying only on self-cleaning filtration can be ecologically and due to the accumulated biowaste something that should be paid special attention to.

#### 5.3.1 Seawater filtration methods

Seawater is taken from the deep sea, so seawater is not what we are used to use, for example in the condensate circuits of power plants. The quality of the seawater must be considered in the filter choices, as well as the location of the seawater filter, whether the seawater filter is at the heat pump plant or on the seabed. The flow of seawater would also be massive, like the seawater system of nuclear power plants. The total seawater flow is approx. 160,000 m<sup>3</sup> / h. What makes filtration difficult is that the filters are located 17-27 km away and at a depth of 50-70 meters, or the filtration is located at a heat pump plant that is approx. 60 meters below ground. Seawater is brought to the plant in a pipe/tunnel and the pipe is full of water, i.e. it is not in open flow. There are for example traveling band screen and Multi-disc screen systems, but the water is not intended to be brought to the surface of the earth to be filtered, these systems do not work on the ground because the seawater flow is not open flow. The heat pump plant is located at a depth of 60 meter, so hydrostatic pressure prevails there, and the filters must be tight and pressure-resistant (pressure class PN10 or PN16). This pressure

requirement can also be too high for most of the drum filters, but there are pressure drum filters from a supplier Andritz, that work at 10 bar.

There are three different ways to take in seawater from a filtration point of view:

- an open hole in the seabed without filter, and carry out coarse and fine filtration at the heat pump plant,
- coarse net on the seabed, and coarse and/or fine filtration (depend seabed coarse net hole size) at the heat pump plant,
- or a filter on the seabed and fine filtration at the heat pump plant.

The choice of filtering is influenced by e.g. organisms, seawater purity, maintenance needs, size class, price and existing technology. Following section describes the seawater filter solutions. In this study the intention is to utilize the heat of deep seawater during the coldest times of the year, so surface intake is not discussed.

#### 5.3.1.1 Seawater intake without subsea filtration

Offshore velocity cap intakes are used for large flows. The cover placed over the intake pipe is called a "velocity cap", it is the most common design type for offshore intake. The cover turns the vertical flow into a horizontal one, which reduces the fish getting caught in the flow at the intake opening. It has been found that fish avoid rapid changes in horizontal flow and caps have reduced fish entrainment by 80-90% at two California power plants and 50-62% at two New England power plants. (Pankratz, 2022) This cap has only been shown to reduce fish entering the intake, but fish can still enter the intake. This works better for some species of fish. Acoustic and optical (e.g. flashing lights or air bubbles) repellents also exist and are used to prevent fish from entering the intake, but their effectiveness has been shown to be limited and species-specific. (Brandt, 2017)

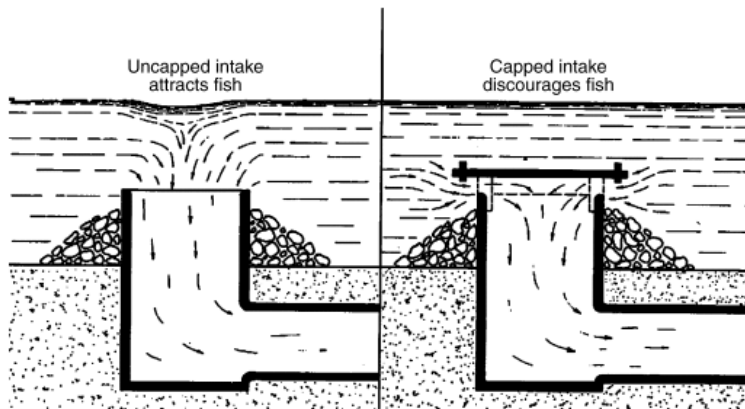


Figure 51 The difference in intake velocity between capped and uncapped cooling water intakes (Brandt, 2017)

Water is brought to the heat pump plant through the offshore intake structure and a tunnel.

The Structures includes:

- offshore velocity cap (with or without coarse screen);
- tunnel (and pipelines);
- bed protection around the intake structure;
- onshore reception pipe/chamber for incoming water;
- coarse and fine screening;
- isolating structures for dewatering the onshore structure for maintenance;
- and seawater pumps for seawater heat pump plant.

The threshold of the waterway intake should be above the seabed level by sufficient distance to ensure that the sediment is not drawn in with the flow to the heat pump plant during larger seawater flowrates or storms. Where necessary the bed should be suitably protected with gravel or rock. Coarse screening on the intake requires regular inspection and maintenance to ensure there is no growth or damage, and the structures should be such that it can be easily removed for maintenance. (Brandt, 2017) Even though the water intake is 50-70 meters below sea level, the seawater maximum flow is approx. 29-32 cm/s and an average flow is approx. 3.5-5.8 cm/s. (Helen internal documents, 2022)

The incoming flow velocity must be less than 0,15 m/s. A typical intake structure is shown in figure 52. The width ( $W$ ) of the threshold must be at least 1,5 times the height ( $H$ ) of the opening. (Brandt, 2017)

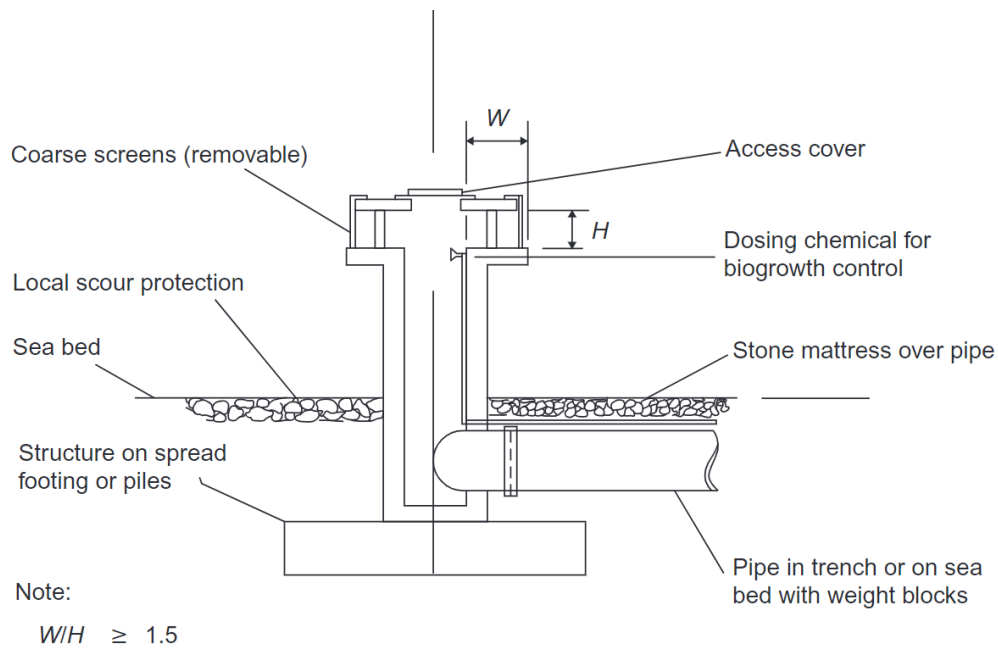


Figure 52 Velocity cap type intake for offshore use (Brandt, 2017)

### 5.3.1.2 Subsea filtration

At the subsea filtration can be done using a passive screening system. Passive screens are static devices using wedge wire or perforated cling free plates mounted in cylindrical cans or polyhedral units (Taprogge/Tapis type). This Taprogge system will be introduced later in this study and will be used as an example. These filters have no moving parts and those seal out debris and aquatic life. In static water or where the flow rate is low, as in this case with seawater, compressed air backflushing should be considered. Backflushing with compressed air would remove the debris that has accumulated in the filter. Such cleaning does not completely remove seaweeds or fibrous material that has accumulated in the net. Therefore, care must be taken to ensure that the sieve units can be removed and cleaned if the back-flushing is not able to remove all the dirt. A compressed air backwash system can be challenging in some places due to noise, safety or local recreational use. Therefore, several

small units may be better than one large one. But this should always be investigated on a case-by-case basis. Air bubbles can reduce the buoyancy of a floating object; therefore, it would be necessary to plan a protection zone in the affected area. (Brandt, 2017)

In the section 3.7. it was said that sea pox larvae attach in summer, when the surface water temperature is around 18 °C. Also, the sea pox larvae live from the water surface to a depth of about 15 meters. Sea pox does not multiply at low temperatures (5-10 °C). Based on these findings, sea pox should not become a problem with subsea filters/nets. Surface water intake is used in summer, so sea pox must be cleaned from surface filters/nets one in the year.

In Finland, all professional divers have that 50-meter working limit and the maximum diving time for one dive to this depth is 5-10 minutes. For example, a group of three divers may be on consecutive dives for 15-30 minutes, followed by a surface time of 4-5 hours. This can be followed by one additional dive with a dive time of about 15 minutes for three people. The third dive cannot be performed during the same day. Increasing the diving group gives a diving time of about 5-10 minutes per person. For this reason, it is a good idea to design the structures simple to install and maintain as possible. The world is dived to a depth of 70 meters, for example in Norway, England and Germany. These are saturation diving companies. (Onjukka, 2022)

Below is a sketch of Taprogge's filter solution (figures 53 and 54). A sufficient number of Tapis filters have been installed on the seabed to keep the flow rate low enough so that the fish do not get caught in the filter net. An air backwash system is connected to the filters, which gives air pressure shocks to clean the filter mesh. The design of the compressed air system must consider the distance of many kilometers from the shore and the sea depth of tens of meters.



Figure 53 Seawater filter system from Taprogge (Gille, 2022)

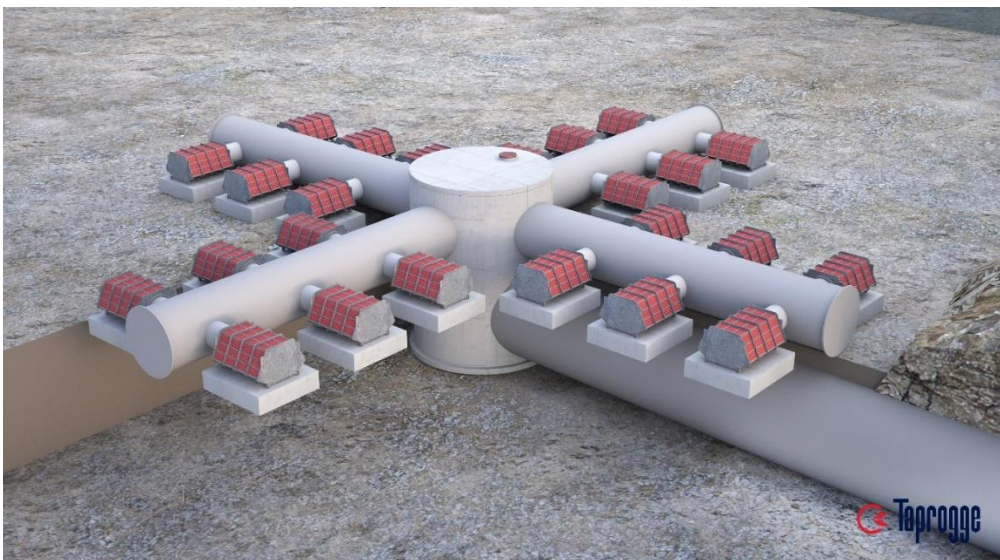


Figure 54 Seawater filter system from Taprogge (Gille, 2022)

There are also tubular filtration solutions for the seabed. Figure 55 shows an illustrative picture of a tubular filter. These have the same fouling problems as the filter solutions mentioned above, and an air backwash system is recommended. Filters of this type also have the goal of keeping the fish in the sea.

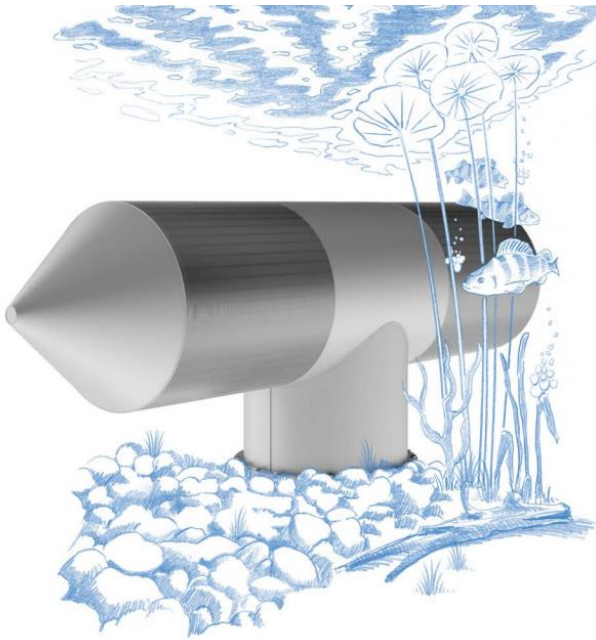


Figure 55 Subsea filtration (Andritz, 2022)

### 5.3.1.3 Seawater filters at the facility

Seawater filtration removes particles from the water that would otherwise cause blockages. Heat exchangers clog easily and lose efficiency, especially in terms of heat transfer and pressure losses. If there was coarse filtration in the seawater intake channel, it may not be sufficient for screening the sand/stone, algae, mussels, and other marine animals contained in the seawater. Without proper filtering, the heat exchangers can become completely blocked and it can even cause device breakdowns. As mentioned earlier, there are active and passive filters. The active filter automatically cleans, and it is a good solution in this case, because the plant has electricity easily available and we want to avoid additional downtime due to clogging of the filters.

The hole size of the filter depends on the desired quality of seawater purity. The generally used minimum hole size is about 1,5...2 mm. A smaller hole size can cause a pressure difference that is too large when the filter gets fouled and there is a risk of the plate tearing and breaking. Heat pump shell-and-tube evaporators often have an inner tube diameter of about 18...25 mm. In this case, filters with a hole size of 5-10 mm are sufficient. The main thing is that a piece of the right size does not get into the heat transfer pipe, causing the pipe

to get stuck. The plate gaps of plate heat exchangers are usually around 2 mm, in which case the hole size of the filter must be less than 2 mm. (Nojonen, 2022)

Many different manufacturers have filters intended for the seawater process, but Taprogge's solution is used as an example. Taprogge has a combined system with seawater filters and a pipe cleaning system for a shell-and-tube heat exchanger. This system can be obtained even for very large water flows, up to 90,000 m<sup>3</sup>/h. The Taprogge ball cleaning system is used, for example, in power plant condensers and heat pump evaporators. In this case, the total water flow is approx. 160,000 m<sup>3</sup> / h, which is distributed over several heat pumps, so a sufficiently large tube cleaning system is available. The water goes to a seawater filter, which automatically removes solids. The water that passed through the filter goes to the evaporator, where is the tube cleaning system. In a tube cleaning system, taprogge balls are fed into a stream of water before to heat exchanger. The system consists of a recirculation pump, a ball collector and piping and the system is controlled by programmable logic. Figure 56 shows the operating principle of the cleaning system and the figure 57 seawater filter structure. Flow is an important factor in the sizing of a tube cleaning system. When the flow rate is higher than the dimensioned, the balls can enter the sea through the ball collector. If the flow rate is too low, the balls can get stuck in the tubes. Taprogge balls are defined according to the application. The determination is influenced by water quality. The balls can also be changed according to the season, if the flow rate is lower in summer, slightly smaller balls can be put in the system. (Taprogge Group, 2022)

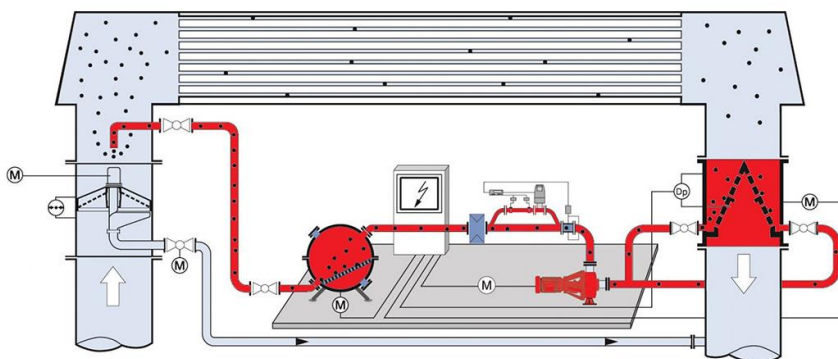


Figure 56 Tube cleaning system PR-BW 800 (Taprogge Group, 2022)

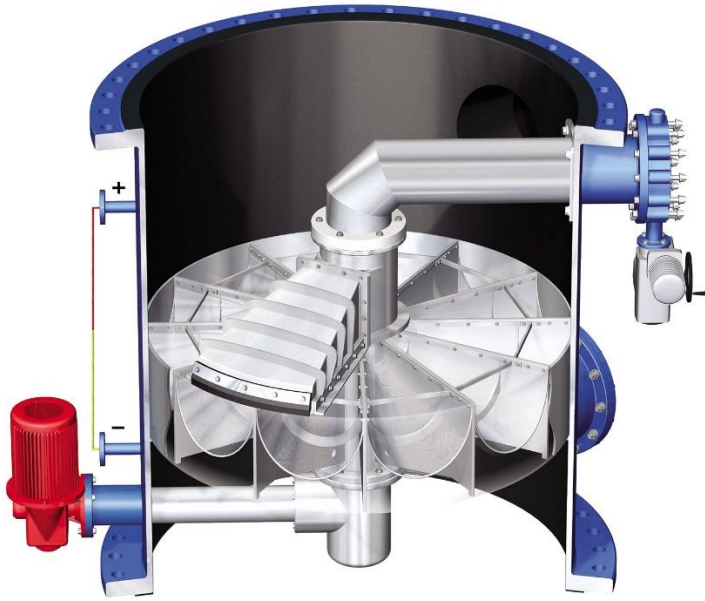


Figure 57 Seawater filter PR-BW 800 (Taprogge Group, 2022)

## 6 Conclusions

The properties of the seawater in the Baltic Sea, such as temperature and salinity, have an influence on the design of the seawater heat pump plant. When the seawater is at the coldest 2-0 degrees, even tenths of the temperature matter. The research questions were; challenges posed by fouling in the seawater process and challenges posed by cold seawater and freezing in the heat pump process. The seawater temperature at a depth of 50-70 meters can go low as 2 and 0,5 degrees in the Baltic Sea Gulf of Finland. Then the seawater is already close to the freezing point when it arrives at the heat pump. Salinity varies with depth, seasons and the physics of the Baltic Sea. Baltic Seawater is brackish water and the salt content at depths of 50-70 meters is about 5-8 ‰ and sometimes even lower. Salinity affects the freezing point and by calculation the freezing point of Gulf of Finland seawater is -0,3...-0,5 degrees. The heat pump plant is designed to be placed underground, where the seawater has an estimated pressure approx. 10 bar. However, pressure does not affect the freezing point as much as salt, but pressure also has a small effect, for example, with a salt concentration of 5‰, seawater freezes at air pressure at about -0,3 degrees, when the pressure is 10 bar, it freezes at about -0,35 degrees.

Freezing can be prevented in a heat pump by using a separate intermediate circuit between the seawater exchanger and the evaporator. With the intermediate circuit the risk of freezing is transferred to the seawater exchanger from the evaporator, where the glycol with negative temperature enters. The evaporator would also not get unclean as easily and it would be possible to make the evaporator from cheaper material. However, the glycol circuit would be massive and would increase investment costs and the seawater heat exchangers would cause more losses and even a small amount of energy should be recovered. It is more reasonable to connect the evaporator directly to the sea, which would save project from extra glycol circuits and temperature losses. For these reasons, it is compared different kind of heat exchangers that are suitable as evaporators for industrial-sized heat pumps and discussed how the evaporators differ from each other in terms of fouling. Evaporators have the good sides and the weaknesses, which makes it hard to say which evaporator is "best".

Four different evaporators were introduced in the study, the shell-and-tube, falling film, diffusion bonded and plate-and-shell heat exchanger. The shell-and-tube heat exchangers are a commonly used technology in industrial-sized heat pumps, and this study revealed why. It is possible to manufacture the tube heat exchanger as a very pressure-resistant structure, even in a large size. The shell-and-tube heat exchanger enables reasonably easy cleaning. The most contaminated liquid should be placed on the side of the pipe so that it is easily accessible for mechanical cleaning. An automatic cleaning system, Taprogge, is available for the tube heat exchanger, so it is not necessarily open or clean chemically as often. The shell-and-tube type heat exchanger is a lot of larger than for example plate-and-shell heat exchanger. The falling film evaporators are used in industrial-sized seawater heat pumps. They are more resistant to freezing than tube heat exchangers, but they need much more space than the other heat exchangers presented in this work. Since falling film heat exchangers are larger the material costs are higher. The diffusion bonded heat exchangers are compact. They take up to 85% less space than falling films heat exchanger. Ultra-high-pressure cleaning uses a diffusion bonded heat exchanger. In ultra-high-pressure cleaning, the high-pressure water is sprayed on fouled areas, and no chemicals are used in this cleaning method. The heat pump requires an interruption of operation and opening the end of the heat exchanger.

The freezing temperature of seawater in the Baltic Sea is approx. -0,3 degrees, so could be imagined that a heat pump could let seawater get that cold. Ice should never form in the

evaporator pipes, i.e. the inner surface of the pipe must not reach below the freezing point. However, it must be remembered that heat exchangers, in this case the evaporator, do not transfer heat with 100% efficiency. The degree of approach is usually a few degrees, in this study the very minimum the degree of approach is studied, which is about 0,5 degrees. In addition, when a safety tolerance for freezing of 0,5 to 0,7 degrees is taken, eventually the minimum seawater temperature rises to 0,7 to 0,8 degrees, depending on the salinity of the seawater. As  $dT$  is reduced, the required mass flow of seawater increases. Also, the full power is not got from the heat pumps when the seawater temperature difference decreases. When seawater is around 0,85 degrees, more district heating can be produced than electricity is consumed. At colder temperatures, other energy production methods can be more efficient.

For further investigation, CFD modeling and an experimental test of freezing should be done. In addition, it would be necessary to find out in more detail the various measurement techniques to detect freezing quickly enough, so that we dare to keep the tolerance for freezing as close to the freezing point as possible. Among the measurements, pressure difference measurement and temperature measurements were mentioned. In addition, the heat pump's compressor should react quickly to a possible freezing situation, for example by increasing the suction pressure.

## References

- Aalto University. 2021. Lecture slide: CHEM-A1120 Virtaustekniikka ja lämmönsiirto. WWW-document. Available at: <file:///C:/Users/knh/Downloads/Virtaustekniikka%20ja%201%C3%A4mm%C3%B6nsiirto%20pruju%202019.pdf> [Accessed 31 May 2022]
- Aalto University. 2021. Lecture slide: Heat transfer. WWW-document. Available at: [https://mycourses.aalto.fi/pluginfile.php/1653745/mod\\_resource/content/4/termis\\_lammon\\_siirto.pdf](https://mycourses.aalto.fi/pluginfile.php/1653745/mod_resource/content/4/termis_lammon_siirto.pdf) [Accessed 31 May 2022]
- Aittomäki, Antero. 2022. Professor of refrigeration technology. Email conversation 24.9.2022.
- Aittomäki, A. 2012. Kylmäteknikka. Porvoo, Bookwell Oy. ISBN: 978-951-96449-7-4
- Akyurt, M., Zaki, G., Habeebullah, B. 2002. Freezing phenomena in ice-water systems. WWW-document. Available at: <https://www.sciencedirect.com.ezproxy.cc.lut.fi/science/article/pii/S0196890401001297?via%3Dihub>
- Alfa Laval Oy. 2022. Email conversation 17.5.2022. [Accessed 21 June 2022].
- Awad, M. M., 2011. Fouling of Heat Transfer Surfaces. Mandoura University. Egypt. WWW-document. Available at: [https://cdn.intechopen.com/pdfs/13202/InTech-Fouling\\_of\\_heat\\_transfer\\_surfaces.pdf](https://cdn.intechopen.com/pdfs/13202/InTech-Fouling_of_heat_transfer_surfaces.pdf) [Accessed 16 June 2022]
- Bott, T.R. 1995. Fouling of Heat Exchangers. Netherlands, Elsevier Science B.V
- Braga, L. B., Milon, J. J. 2012. Visualization of dendritic ice growth in supercooled water inside cylindrical capsules. WWW-document. Available at: <https://www.sciencedirect.com.ezproxy.cc.lut.fi/science/article/pii/S001793101200155X?via%3Dihub> [Accessed 21 June 2022]
- Brandt, M. J. Johnson, K. M. Elphinston, A. J. Ratnayaka, D. D. 2017. Twort's water supply. 7<sup>th</sup> edition. United Kingdom: Elsevier Science & Technology. ISBN: 978-0-08-100025-0.
- Cengel, Y., Boles, M. Kanoglu, M. 2020. Thermodynamics: An Engineering Approach. New York, McGraw-Hill.

Ebbing, D. Gammon, S. 2017. General Chemistry. Boston: Cengage Learning. ISBN: 9781305580343.

Gille, Detlef. 2022. TAPROGGE GMBH. Email conversation 8.7.2022.

Gilpin, R. R. 1977. The effects of dendritic ice formation in water pipes. WWW-document. Available at: <https://www.sciencedirect.com/science/article/abs/pii/0017931077900576> [Accessed 18 July 2022].

Hayek, M. Salgues, M. Souche, J. Cunge, E. Giraudel, C. Paireau, O. 2021. Influence of the Intrinsic Characteristics of Cementitious Materials on Biofouling in the Marine Environment. WWW-document. Available at: <https://www.mdpi.com/2071-1050/13/5/2625/htm> [Accessed 19 July 2022]

Heat Transfer Technology. 2022. Falling Film Chiller. WWW-document. Available at: <https://www.htt-ag.com/products/falling-film-chiller/> [Accessed 27 July 2022].

Heatric. 2018. Diffusion Bonding in Compact Heat Exchangers. WWW-document. Available at: <https://www.heatric.com/app/uploads/2018/04/Diffusion-bonding-in-compact-heat-exchangers.pdf> [Accessed 27 May 2022]

Heatric. 2022. Diffusion Bonding Technology. WWW-document. Available at: <https://www.heatric.com/heat-exchangers/features/diffusion-bonding/> [Accessed 27 May 2022].

Helen Oy internal documents. 2022.

Helen Oy, 2022. Helen's seawater heat recovery project progresses. WWW-document. Available at: <https://www.helen.fi/uutiset/2022/helen-kilpailuttaa-allianssikumppanin-merivesij%C3%A4rjestelm%C3%A4n-kehitys-ja-toteutusvaiheisiin> [Accessed 4 April 2022]

Helen Oy, 2022. Meriveden lämmöntalteenotto. WWW-document. Available at: <https://www.helen.fi/helen-oy/energia/kehityshankkeet/biolampolaitokset/meriveden-lammontalteenotto> [Accessed 4 April 2022]

Helsingin kaupunki, 2020. Pääkaupunkiseudun merialueen tila 2018–2019. WWW-document. Available at: <https://www.hel.fi/static/ymk/merialueen-seuranta/viimeisin-yhteenvetoraportti.pdf> [Accessed 4 April 2022]

Institutes of the Faculty of Engineering. 2022. Phase Diagram of Salt Water. WWW-document. Available at: [https://www.tf.uni-kiel.de/matwis/amat/iss/kap\\_6/illustr/i6\\_2\\_2.html](https://www.tf.uni-kiel.de/matwis/amat/iss/kap_6/illustr/i6_2_2.html) [Accessed 4 July 2022]

Itämeri.fi, 2017. Merenpohjan nuoremmat kerrostumat. WWW-document. Available at: [https://www.ostersjon.fi/fi-FI/Luonto\\_ja\\_sen\\_muutos/Ainutlaatuinen\\_Itameri/Merenpohjan\\_nuoremmat\\_kerrostumat](https://www.ostersjon.fi/fi-FI/Luonto_ja_sen_muutos/Ainutlaatuinen_Itameri/Merenpohjan_nuoremmat_kerrostumat) [Accessed 19 July 2022]

Itämeri.fi, 2022. Suolaisuus, lämpötila ja kerrostuneisuus. WWW-document. Available at: [https://itameri.fi/fi-FI/Luonto\\_ja\\_sen\\_muutos/Ainutlaatuinen\\_Itameri/Suolaisuus\\_lampotila\\_ja\\_kerrostuneisuus](https://itameri.fi/fi-FI/Luonto_ja_sen_muutos/Ainutlaatuinen_Itameri/Suolaisuus_lampotila_ja_kerrostuneisuus) [Accessed 11 April 2022]

Itämeri.fi, 2022. Vedenlaatu: Happipitoisuus. WWW-document. Available at: [Itämeren lämpötilaa seurataan jatkuvasti - itämeri.fi \(ostersjon.fi\)](https://itameri.fi/fi-FI/lamportila_seurataan_jatkuvasti_-_itameri.fi_(ostersjon.fi)) [Accessed 6 April 2022]

Jyväskylän yliopisto. 2010. Jäätymispisteen alenema. WWW-document. Available at: <https://koppa.jyu.fi/avoimet/kemia/kems448/suomeksi/ohjeet/liuokset/jaatumispiste> [Accessed 22 April 2022]

Komulainen, Antti. 2022. Process specialist, Helen Oy, Helsinki. Conversation 31.3.2022.

Laitinen, Timo. 2022. Senior Lecturer, Metropolia University of Applied Sciences, Helsinki. Conversation 1.6.2022.

Luontoportti. 2022. Merirokko. WWW-document. Available at: <https://luontoportti.com/t/2988/merirokko> [Accessed 18 July 2022]

Mullin, J. W. 2001. Crystallization. London: Elsevier Science & Technology. ISBN: 9780080530116.

Myrberg, Kai., Leppäranta, Matti. Kuosa, Harri. 2006. [Itämeren fysiikka, tila ja tulevaisuus. Helsinki, Yliopistopaino.](#) ISBN: 951-570-654-8.

Myrkyttömästivesillä.fi. 2022. Puhdistus. WWW-document. Available at: <https://www.myrkyttomastivesilla.fi/puhdistus> [Accessed 18 July 2022]

Noponen, Veijo. 2022. Planning Manager. Helen Oy, Helsinki. Conversation 26.9.2022.

Omt-triaca. 2022. Industrial Refrigerating Plants Constructor for Food and Dairy Industries. WWW-document. Available at: <https://www.omt-triaca.com/es/falling-film-baudelot-cooler/> [Accessed 23 June 2022]

Onjukka, Jorma. 2022. Commercial Diver, Sukelluspalvelu Stella Maria, Varkaus. Email conversation 20.6.2022.

Outokumpu, 2009. Corrosion Handbook. Espoo, Outokumpu Oyj.

Pankratz, T. 2022. An Overview of Seawater Intake Facilities for Seawater Desalination. WWW-document. Available at: <https://texaswater.tamu.edu/readings/desal/seawaterdesal.pdf> [Accessed 19 July 2022]

retkikartta.fi. 2022. WWW-document. Available at: <https://retkikartta.fi/> [Accessed 19 July 2022]

Saari, Jussi. 2010. Heat Exchanger Thermal Design Guide. Lappeenranta University of Technology. ISBN 978-952-214-968-8

Suomen ympäristökeskus. 2020. Suomenlahden vesimassa on sekoittunut ja happitilanne on parempi kuin vuosiin. WWW-document. Available at: [https://www.syke.fi/fi-FI/Ajankohtaista/Suomenlahden vesimassa on sekoittunut ja%2856296%29](https://www.syke.fi/fi-FI/Ajankohtaista/Suomenlahden-vesimassa-on-sekoittunut-ja%2856296%29) [Accessed 19 July 2022]

[Suomen ympäristökeskus. 2022. Itämeri: Ympäristö ja ekologia.](https://www.syke.fi/download/noname/%7BC0E3E83E-6BEB-489E-939E-06C4B82E1501%7D/97989) WWW-document. Available at: <https://www.syke.fi/download/noname/%7BC0E3E83E-6BEB-489E-939E-06C4B82E1501%7D/97989> [Accessed 13 June 2022]

Taprogge Group. 2022. Type D 2 Strainer Section. WWW-document. Available at: <https://www.taprogge.com/anwendungsfelder-produkte/efficiency-in-energy-and-water-kraftwerke-und-industrie/kuehlrohrreinigung/siebeinrichtung-typ-d2/> [Accessed 2 June 2022]

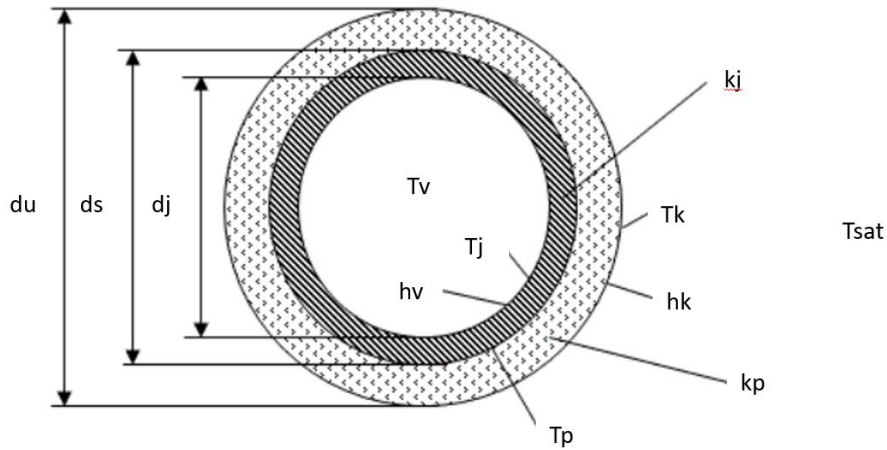
Vahterus. 2022. Interactive model of Vahterus PSHE Fully Welded. WWW-document. Available at: <https://vahterus.com/virtual/products/fully-welded/> [Accessed 13 August 2022].

Vesi.fi. 2019. WWW-document. Available at: <https://www.vesi.fi/vesitieto/vaivaako-happikato/> [Accessed 18 July 2022].

Vieraslajit.fi. 2012. Merirokko. WWW-document. Available at: <https://vieraslajit.fi/lajit/MX.53030> [Accessed 19 July 2022].

VPE. 2022. Diffusion bonded microchannel heat exchangers. WWW-document. Available at: <https://www.vpei.com/diffusion-bonded-microchannel-heat-exchangers/> [Accessed 13 August 2022].

Appendix 1. Example calculation of the heat transfer in evaporator pipe



$$T_{sat} = \text{saturated refrigerant temperature} = -0,6 \text{ } ^\circ\text{C}$$

$$T_{v1} = \text{water inlet temperature} = 2 \text{ } ^\circ\text{C}$$

$$T_{v2} = \text{water outlet temperature} = -0,3 \text{ } ^\circ\text{C}$$

$$\Delta T_{in} = 2 \text{ } ^\circ\text{C} - (-0,6 \text{ } ^\circ\text{C}) = 2,6 \text{ } ^\circ\text{C}$$

$$\Delta T_{out} = -0,3 \text{ } ^\circ\text{C} - (-0,6 \text{ } ^\circ\text{C}) = 0,3 \text{ } ^\circ\text{C}$$

$$\Delta T_m = \text{mean temperature difference} = \frac{\Delta T_{in} - \Delta T_{out}}{\ln(\Delta T_{in} / \Delta T_{out})} = \frac{2,6 \text{ } ^\circ\text{C} - 0,3 \text{ } ^\circ\text{C}}{\ln(2,6 \text{ } ^\circ\text{C} / 0,3 \text{ } ^\circ\text{C})} = 2,76 \text{ } ^\circ\text{C}$$

$$k_j = \text{ice thermal conductivity} = 2,22 \text{ W/mK}$$

$$k_p = \text{pipe thermal conductivity} = 19 \text{ W/mK}$$

$$k_v = \text{pipe thermal conductivity} = 0,56 \text{ W/mK}$$

$$h_k = \text{refrigerant heat transfer coefficient} = ?$$

$$d_j = \text{ice layer inside diameter} = 0,015 \text{ m}$$

$$d_s = \text{pipe inside diameter} = 0,019 \text{ m}$$

$$d_u = \text{pipe outside diameter} = 0,021 \text{ m}$$

$$\dot{V} = \text{volume flow} = 0,000269 \frac{\text{m}^3}{\text{h}} \rightarrow u = \text{flow velocity} = 1,52 \text{ m/s} \rightarrow \dot{m} = \text{massflow} = 0,269 \text{ kg/s}$$

$$\nu = \text{water kinematic viscosity} = 0,0000017919 \text{ m}^2/\text{s}$$

$$\mu = \text{water dynamic viscosity} = 0,001788 \text{ Pa} \cdot \text{s}$$

$$c_p = \text{specific heat capacity} = 4184 \text{ J/kgK}$$

$$Q = \text{heat transfer rate} = \dot{m} \cdot c_p \cdot \Delta T = 0,269 \text{ kg/s} \cdot 4184 \text{ J/kgK} \cdot (2 \text{ }^\circ\text{C} - (-0,3 \text{ }^\circ\text{C})) \\ = 2588,6 \text{ W}$$

$$G = \text{conductance} = \frac{Q}{\Delta T_m} = \frac{2588,6 \text{ W}}{2,76 \text{ }^\circ\text{C}} = 937,4 \text{ W/}^\circ\text{C}$$

$$Pr = \frac{\mu \cdot c_p}{k_v} = \frac{0,001788 \text{ (Pa} \cdot \text{s)} \cdot 4184 \text{ J/kgK}}{0,56 \text{ W/mK}} = 13,36$$

$$Re = \frac{u \cdot d_j}{\nu} = \frac{1,52 \frac{\text{m}}{\text{s}} \cdot 0,015 \text{ m}}{0,0000017919 \frac{\text{m}^2}{\text{s}}} = 12723,9$$

$$Nu = \frac{\left(\frac{f}{8}\right) (Re - 1000) Pr}{1 + 12,7 \left(\frac{f}{8}\right)^{\frac{1}{2}} (Pr^{\frac{2}{3}} - 1)} = 131,2$$

$$f = (0,79 \cdot \ln(Re) - 1,64)^{-2} = (0,79 \cdot \ln(12723,9) - 1,64)^{-2} = 0,03139$$

$$h_v = \text{water heat transfer coefficient} = \frac{Nu \cdot k_v}{d_j} = \frac{131,2 \cdot 0,56 \text{ W/mK}}{0,015 \text{ m}} = 4898,75 \text{ W/m}^2\text{K}$$

$$R_s = \text{resistance from the water to the outer surface of the pipe} = \frac{1}{\pi * dj * hv} + \frac{\ln\left(\frac{ds}{dj}\right)}{2 * \pi * kj} + \frac{\ln\left(\frac{du}{ds}\right)}{2 * \pi * kp}$$

$$= \frac{1}{\pi * 0,015 \text{ m} * 4898,75 \frac{W}{m^2K}} + \frac{\ln\left(\frac{0,019 \text{ m}}{0,015 \text{ m}}\right)}{2 * \pi * 2,22 \frac{W}{mK}} + \frac{\ln\left(\frac{0,021 \text{ m}}{0,019 \text{ m}}\right)}{2 * \pi * 19 \frac{W}{mK}} = 0,022 \frac{1}{W/mK}$$

$$R_u = \text{resistance from the refrigerant to the outer surface of the pipe} = \frac{1}{\pi * dj * hk}$$

$$\frac{T_v - T_k}{R_s} = \frac{T_k - T_{sat}}{R_u}$$

$$hk = C2 * (T_k - T_{sat})^{2,922}$$

Used as  $T$  is the average temperature

$$\rightarrow \frac{T_v - T_k}{R_s} = \frac{T_k - T_{sat}}{\frac{1}{\pi * dj * hk}} \rightarrow \frac{T_v - T_k}{R_s} = \frac{T_k - T_{sat}}{\frac{1}{\pi * dj * (C2 * (T_k - T_{sat})^{2,922})}}$$

$$\rightarrow \frac{1,15 \text{ }^\circ\text{C} - T_k}{0,022 \frac{1}{W/mK}} = \frac{T_k - (-0,6 \text{ }^\circ\text{C})}{\frac{1}{\pi * 0,015 \text{ m} * (6 * (T_k - -0,6 \text{ }^\circ\text{C})^{2,922})}}$$

$$\rightarrow hk = 28,3 \text{ W/m}^2\text{K and } T_k = 1,10 \text{ }^\circ\text{C}$$

$$R_u = \frac{1}{\pi * dj * hk} = \frac{1}{\pi * 0,015 \text{ m} * 22,3 \text{ W/m}^2\text{K}} = 0,274 \frac{1}{W/mK}$$

$$U = \frac{1}{R_{tot}} = \frac{1}{0,274 \frac{1}{W/mK} + 0,022 \frac{1}{W/mK}} = 3,379 \frac{W}{mK}$$

$$L = \frac{G}{U} = \frac{937,4 \text{ W/}^\circ\text{C}}{3,379 \frac{W}{mK}} = 277 \text{ m}$$